1-1-2016

Unravelling the mechanism of TrkA-induced cell death by macropinocytosis in medulloblastoma Daoy cells

Chunhui Li
Robarts Research Institute

James I.S. MacDonald
Robarts Research Institute

Asghar Talebian
Western University

Jennifer Leuenberger
Western University

Claudia Seah
Robarts Research Institute

See next page for additional authors

AMERICAN SOCIETY FOR MICROBIOLOGY | Molecular and Cellular Biology

Unravelling the Mechanism of TrkA-Induced Cell Death by Macropinocytosis in Medulloblastoma Daoy Cells

Chunhui Li,[a] James I. S. MacDonald,[a] Asghar Talebian,[c]* Jennifer Leuenberger,[c]* Claudia Seah,[a] Stephen H. Pasternak,[a,b] Stephen W. Michnick,[e] Susan O. Meakin[c,d]

Robarts Research Institute[a] and Department of Clinical Neurological Sciences,[b] Schulich School of Medicine, Western University, London, Ontario, Canada; Department of Biochemistry[c] and Graduate Program in Neuroscience,[d] Western University, London, Ontario, Canada; Département de Biochimie, Université de Montreal, Montreal, Quebéc, Canada[e]

Macropinocytosis is a normal cellular process by which cells internalize extracellular fluids and nutrients from their environment and is one strategy that Ras-transformed pancreatic cancer cells use to increase uptake of amino acids to meet the needs of rapid growth. Paradoxically, in non-Ras transformed medulloblastoma brain tumors, we have shown that expression and activation of the receptor tyrosine kinase TrkA overactivates macropinocytosis, resulting in the catastrophic disintegration of the cell membrane and in tumor cell death. The molecular basis of this uncontrolled form of macropinocytosis has not been previously understood. Here, we demonstrate that the overactivation of macropinocytosis is caused by the simultaneous activation of two TrkA-mediated pathways: (i) inhibition of RhoB via phosphorylation at Ser^{185} by casein kinase 1, which relieves actin stress fibers, and (ii) FRS2-scaffolded Src and H-Ras activation of RhoA, which stimulate actin reorganization and the formation of lamellipodia. Since catastrophic macropinocytosis results in brain tumor cell death, improved understanding of the mechanisms involved will facilitate future efforts to reprogram tumors, even those resistant to apoptosis, to die.

Medulloblastomas (MEDs) and neuroblastomas (NBs) represent two of the most common childhood neoplasias of the central and peripheral nervous systems (1, 2). MEDs arise from progenitor cells in the cerebellum (3) while NBs arise from undifferentiated sympathoadrenal cells of neural crest origin (2, 4). In general, the age of onset for both MEDs and NBs is an important determinate of the final prognosis, with complete regression often being reported in children under 1 year of age. In contrast, tumors that arise in older children often become metastatic and highly resistant to conventional therapies (5). Two markers, the expression of which correlate with positive prognosis in both MEDs and NBs, are the closely related receptor tyrosine kinases (RTKs) TrkA and TrkC (5, 6, 7). In contrast, expression of TrkB correlates with enhanced drug resistance, MYCN expression, and angiogenesis (5) and is a poor prognostic predictor of NBs, and it also facilitates cell survival and proliferation in MEDs (8).

The relationship between Trk receptor expression and the final prognostic outcome has been linked to the induction of cell death. In many instances, in both primary as well as established MED, NB, and glioblastoma (GB) cell lines, expression of either TrkA or TrkC has been linked to the induction of either apoptosis or autophagy (1, 9–12). In contrast, we have shown that nerve growth factor (NGF) treatment of MED Daoy cells that overexpress TrkA (Daoy-TrkA) show a dramatic increase in uncontrolled macropinocytosis, causing catastrophic disintegration of cellular membrane integrity, which results in cell death (13). No evidence of apoptosis or necrosis is observed, and although evidence of autophagy is present, small interfering RNA (siRNA)-mediated knockdown of the key autophagy proteins, beclin and Atg5, does not prevent cell death (13).

Macropinocytosis is an actin-dependent, clathrin-independent, endocytic process that can be triggered by external stimuli and serves as a means for cells to take up large amounts of extracellular materials as nutrients (14, 15, 16). Under normal conditions, macropinocytosis can also facilitate receptor-mediated signaling pathways, the entry of viral and bacterial pathogens, and cell motility (16) and is the mechanism by which macrophages and dendritic cells internalize antigens and cellular debris (16, 17). More recently, macropinocytosis has also been shown to facilitate the uptake of amino acids in Ras-transformed pancreatic tumor cells to sustain their uncontrolled proliferation (14). Macropinosomes are generated by the formation of cell surface lamellipodia that fold back on themselves, resulting in large endosomes, which can be larger than 0.2 μm in diameter (18). Under normal physiological conditions, macropinosomes are either recycled back to the cell surface, or they fuse with lysosomes to digest internalized nutrients (15, 16). By comparison, the macropinosomes generated in NGF-treated Daoy-TrkA cells internally fuse, growing uncontrollably larger, and in turn fuse with lysosomes (13). The cells literally drink and eat themselves to death.

In addition to our observations in MEDs, hyperstimulation of macropinocytosis has also been found to result in cell death in some human GB cell lines as well as in other cancer cell lines (19–22). Interestingly, overexpression of oncogenic Harvey-Ras

Received 4 May 2016 **Returned for modification** 19 July 2016
Accepted 29 July 2016

Accepted manuscript posted online 8 August 2016

Citation Li C, Macdonald JIS, Talebian A, Leuenberger J, Seah C, Pasternak SH, Michnick SW, Meakin SO. 2016. Unravelling the mechanism of TrkA-induced cell death by macropinocytosis in medulloblastoma Daoy cells. Mol Cell Biol 36:2596–2611. doi:10.1128/MCB.00255-16.

Address correspondence to Susan O. Meakin, smeakin@uwo.ca.

* Present address: Asghar Talebian, University of Texas Southwestern Medical Center, Dallas, TX, USA; Jennifer Leuenberger, Canadawide Scientific, Ottawa, Ontario, Canada.

Supplemental material for this article may be found at http://dx.doi.org/10.1128/MCB.00255-16.

(H-Ras), has been shown to drive cell death by macropinocytosis in the GB cell line, U251 (13, 20), by a mechanism that is dependent upon activation of the GTPase Rac1 and the inactivation of Arf6 (23).

Here, we characterize the signaling mechanisms that drive TrkA-dependent cell death by macropinocytosis in Daoy cells. We find that, similar to U251 cells, induction of macropinocytosis-dependent cell death requires the activation of H-Ras; however, unlike U251 cells, it does not depend on the activation of Rac1 or Cdc42.

Moreover, we find that overexpression of constitutively active (CA) H-Ras alone is sufficient to activate macropinocytosis-dependent cell death. While it may seem surprising that CA-H-Ras can stimulate cell death in a brain tumor cell line, it is important to note that activating mutations of either H-Ras, neuroblastoma-Ras (N-Ras), or Kirsten-Ras (K-Ras) have not been found in cancers of the brain (24, 25). In terms of understanding the mechanisms driving this process, we demonstrate the concomitant requirement of several signaling pathways. First, we find that activation of Src is essential, which is known to precede activation of H-Ras (26), and that this is mediated via the adapter protein FRS2 (fibroblast growth factor receptor substrate 2), not ShcA, which competitively binds to the juxtamembrane phosphorylated tyrosine residue, pTyr$^{490/499}$, on activated TrkA (27). Second, we show that two Rho family GTPases, RhoA and RhoB, are the endpoint effectors and that they serve essential but opposite roles in regulating macropinocytosis. Finally, we have identified an essential role for the serine/threonine kinase casein kinase 1 (CK1) in a mechanism that involves the phosphorylation of RhoB at Ser^{185}. This single event inactivates RhoB (28), releasing actin stress fibers, and enables RhoA to reorganize actin into the lamellipodial extensions required to generate macropinosomes.

MATERIALS AND METHODS

Antibodies and growth factors. The antibodies to β-actin and Arf6 were from Sigma-Aldrich. Antibodies to Cdc42, FRS2, H-Ras, N-Ras, Rap1, RhoB, and Sck (ShcB) were from Santa Cruz Biotechnology. Antibodies to RhoA, phospho-Src (Tyr^{416}), phosphor-Src (Tyr^{547}), and anti-phospho-TrkA (Tyr^{490}) were from Cell Signaling Technology. Antibodies to ShcA, ShcC, and Rac1 were from BD Bioscience. The antibody to K-Ras was from Abcam, and the antibody to v-*src* was from Calbiochem. Horseradish peroxidase (HRP)-coupled secondary antibodies (rabbit anti-mouse and goat anti-rabbit antibodies) were from Jackson ImmunoResearch Labs, Inc., and were used at final concentrations of 1:10,000. Antibodies were used at working concentrations as follows: anti-β-actin (1:10,000), anti-phospho-TrkA (Tyr^{490}) (1:2,000), phospho-Src (Tyr^{416}) (1:5,000), phospho-Src (Tyr^{547}) (1:2,000), anti-ShcA (1:5,000), anti-ShcC (1:10,000), anti-ShcB (1:1,000), anti-FRS2 (1:2,000), anti-v-*src* (1:1,000), anti-glutathione *S*-transferase (anti-GST)–HRP (1:5,000), anti-Ras (1:1,000), anti-Rac (1:1,000), anti-Cdc42 (1:5,000), anti-Arf6 (1:1,000), anti-RhoA (1:1,000), anti-RhoB (1:500), and anti-Rap1 (1:1,000). Nerve growth factor (NGF) was from Harlan Products for Bioscience.

Vectors and cloning. CA-Rac1 (Q^{61}L) was generated by site-directed mutagenesis using *PfuTurbo* (Stratagene). Human H-Ras cDNA was obtained by PCR amplification from human placenta cDNA and subcloned into pEGFP-C1 (where EGFP is enhanced green fluorescent protein). CA-H-Ras (G^{12}V)-EGFP was generated using human CA-H-Ras as a template by site-directed mutagenesis using Pfu Turbo. All other constructs were provided by the following investigators: EGFP-tagged DN (T^{19}L) and CA (Q^{63}L) RhoB from A. Richmond (Vanderbilt University School of Medicine, TN); EGFP-tagged DN (T^{66}N) and CA (Q^{111}L) Rab34 from T. Endo (Chiba University, Chiba, Japan); EGFP-tagged CA (G^{12}V) and DN (T^{17}N) Cdc42, DN (S^{17}N) Rac, DN (K^{44}A) dynamin 2, DN (T^{31}N) Arf1, yellow fluorescent protein (YFP)-tagged DN (N^{19}L) RhoA, DN (S^{34}N) Rab5, DN (T^{22}N) Rab7, and EGFP-tagged clathrin from S. Ferguson (University of Ottawa, Ontario, Canada); EGFP-tagged DN (S^{17}N) and CA (G^{12}V) Rap1b from P. Stork (Vollum Institute, OR); pYFP-tagged DN (S^{147}A) CtBP1/BARS from Alberto Luini (Institute of Protein Biochemistry, NRC, Naples, Italy); EGFP-tagged DN (T^{17}N) and CA (Q^{61}L) Arf6 from J. Donaldson (NIH, MD); constructs encoding the pleckstrin homology (PH) domains of phospholipase Cδ (PLCδ) and AKT fused with EGFP as well as the Ras binding domain (RBD) cysteine-rich domain (CRD) of c-Raf-1 fused with EGFP from T. Balla (NIH, MD); EGFP-tagged cRaf-1 CRD (R^{89}A) mutant from Y. Sako (RIKEN ASI, Japan); EGFP-tagged DN-Src516 (residues 1 to 516) from N. Yamaguchi (Chiba University, Japan); EGFP-RhoB (S^{185}A) from A. Pradines (INSERM, Toulouse, France), and the GFP-RhoA binding domain of rhotekin to visualize active RhoA (GFP-rGBD) from W. Bement (Addgene 26740 and 26732). pGex vectors expressing GST fusions encoding binding domains for specific GTPases were obtained from the following investigators: RBD of c-Raf (Raf-RBD) from D. Shalloway (University of California, Berkeley, CA); Cdc42/Rac-interacting binding (CRIB) domain of p21-activated kinase 1 (Pak1) from A. Hall (Memorial Sloan-Kettering Cancer Center, NY); RBD of RalA (RalGDS-RBD) from P. Stork (Vollum Institute, OR); Rho binding domain of rhotekin from A. Richmond (Vanderbilt University, TN); and the N-terminal GAT (NGAT) domain of the Golgi compartment-localized gamma ear-containing Arf-binding protein 3 (GGA3), which binds activated Arf6, from M. Park (McGill University, Montreal, CA).

Cell culture and transfections. Daoy-TrkA cells were provided by V. Lee (University of Pennsylvania, PA) and maintained in Dulbecco's minimal Eagle medium (DMEM) supplemented with 10% fetal bovine serum, 100 μg/ml gentamicin sulfate, and 100 μg/ml G418. Daoy cells were grown in the same medium without G418. Cells were routinely transfected with 4 to 10 μg of plasmid or 20 nM siRNA using Lipofectamine 2000 (Life Technologies) or DreamFect Gold (OZ Biosciences) according to the specifications of the manufacturer.

Small interfering RNAs. Validated or sequence-specific siRNAs were generated and purchased from Life Technologies against the following targets: (i) human H-Ras (validated stealth siRNA VHS40291), (ii) human FRS2 (sense, CUG GCU AUG ACA GUG AUG AAC GAA G; antisense, CUU CGU UCA UCA CUG UCA UAG CCA G), (iii) Src (sense, AAC AAG AGC AAG CCC AAG GAU; antisense, AUC CUU GGG CUU GCU CUU GUU) (29), (iv) human ShcA (silencer select 4390827; sense, CUA CUU GGU UCG GUA CAU GGG; antisense, CAU GUA CCG AAC CAA GUA GGA), (v) human Rac1 (sense, UUU GAC AGC ACC GAU CUC UUU CGC C; antisense, GGC GAA AGA GAU CGG UGC UGU CAA A), (vi) human Cdc42 (sense, UCC UUU CUU GCU UGU UGG GAC UCA A; antisense, UUG AGU CCC AAC AAG CAA GAA AGG A) (30), (vii) human RhoB (sense, CCG UCU UCG AGA ACU AUC UUU; antisense, AGA UAG UUC UCG AAG ACG GUU), and (viii) a stealth control (sense, GAG UCG ACC UAG UGU AAC ACC GAC A; antisense, UGU CGG UGU UAC ACU AGG UCG ACU C). A Cy3-labeled negative-control siRNA (Life Technologies) was cotransfected with test siRNAs to monitor transfection efficiency.

Inhibitor/dyes. Daoy-TrkA cells were pretreated with the following inhibitors 1 h prior to NGF stimulation (100 ng/ml) unless otherwise stated: 40 μM concentration of the CK1 inhibitor (D4476; Calbiochem), 5 to 10 μM concentration of the Rac1 inhibitor EHT1864 (Tocris Bioscience), and 2 μg/ml of the Rho inhibitor CT04 (Cytoskeleton, Inc.). The Src inhibitor PP2 (Sigma-Aldrich) was used at the concentrations indicated. Dimethyl sulfoxide (DMSO) was used as a negative control. Alexa Fluor 546-dextran, Alex Fluor 488-dextran, and Alexa Fluor 546-transferrin (Life Technologies) were used at a final concentration of 5 μg/ml (dextran) or 50 μg/ml (transferrin).

GTPase binding assays. Bacteria expressing pGex2T, pGex2T-Pak-CRIB, pGex-Raf1-RBD, pGex-RalGDS-RBD, pGex-Rhotekin-RBD, and

pGex-GGA3-NGAT were grown in 50 ml of Luria broth (LB) with 50 μg/ml ampicillin for 16 h at 37°C and then added to 500 ml of LB with 50 μg/ml ampicillin and grown to an optical density at 600 nm (OD_{600}) of 0.8 to 1.0. Cultures were induced with isopropyl-β-D-thiogalactopyranoside (IPTG; 0.2 mg/ml) for 2 h at 37°C, centrifuged at 5,000 rpm for 10 min (4°C), resuspended in 10 ml of 1× phosphate-buffered saline (PBS), and frozen at −80°C. Pellets were resuspended in 20 ml of resuspension buffer (25 mM Tris-Cl, pH 7.5, 5 mM EDTA, pH 8.0, 150 mM NaCl, 1 mM phenylmethylsulfonyl fluoride [PMSF], 1 μg/ml leupeptin). Cells expressing the Pak-CRIB domain were lysed by two passages through a prechilled French press at 20,000 lb/in^2. Triton X-100 was added to a final concentration of 1%, and the sample was rotated for 30 min at 4°C. All other GST fusions were resuspended as described above and lysed directly by the addition of Triton X-100 to a final concentration of 1%. Samples were centrifuged at 14,000 rpm for 10 min at 4°C. Washed glutathione-agarose (500 μl) (Sigma-Aldrich) was added to the supernatant, and the mixtures were incubated for 16 h at 4°C, followed by three washes with 10 ml of 1× PBS and resuspended in 250 μl of interaction buffer (20 mM HEPES, 150 mM NaCl, 0.05% NP-40, 10% glycerol, 1 mM PMSF, 1 μg/ml leupeptin). To measure changes in GTP activation, Daoy-TrkA cells were left untreated or stimulated with NGF (100 ng/ml) for 10 min, 6 h, 12 h, and 24 h. Prior to lysis, cells were placed on ice, washed with ice-cold phosphate-buffered saline (PBS), lysed in 500 μl of interaction buffer (containing 100 μM GTPγS, 10 μg/ml aprotinin, 2 μg/ml leupeptin, and 1 mM PMSF) for 2 min, and lysates were centrifuged at 10,000 rpm for 10 min at 4°C. Protein concentrations of lysates were determined with a detergent-compatible (DC) protein assay kit (Bio-Rad), and the main lysates were flash frozen in liquid nitrogen and stored at −80°C until use. Purified GST fusion proteins (approximately 30 μg) were added to 500 to 1,000 μg of unstimulated and NGF-stimulated Daoy-TrkA lysates and incubated at 4°C for 16 h (1 h for RhoA). Samples were pelleted at 14,000 rpm at 4°C and washed twice with interaction buffer. Laemmli sample buffer with 100 mM dithiothreitol (DTT) was added, and samples were heated at 70°C for 10 min. Proteins were analyzed by 12% SDS-PAGE and blotted with anti-GST–HRP (1:5,000), anti-H-Ras (1:1,000), anti-Rac1 (1:1,000), anti-Cdc42 (1:5,000), anti-Arf6 (1:1,000), anti-RhoB (1:500), anti-RhoA (1:1,000), and anti-Rap1 (1:1,000) antibodies. Lysates from each time point (25 μl) were also assayed for changes in the expression of each GTPase relative to β-actin as a control.

Immunoprecipitation and Western blotting. Daoy-TrkA cells were stimulated with NGF (100 ng/ml), washed twice with ice-cold PBS containing 1 mM sodium orthovanadate, and lysed in NP-40 lysis buffer (1% NP-40, 137 mM NaCl, 10% glycerol, 1 mM EDTA, 50 mM Tris-HCl, pH 8.0) containing 1 mM sodium orthovanadate, 10 mM NaF, 10 μg/ml aprotinin, 2 μg/ml leupeptin, and 1 mM PMSF. Clarified supernatants were collected by centrifugation, and lysates (500 μg) were immunoprecipitated with an antibody to TrkA and GammaBind Plus Sepharose (Amersham Pharmacia Biotech). Immune complexes were collected by centrifugation after an overnight incubation at 4°C, washed, and resuspended in SDS-PAGE sample buffer. Immunoprecipitated proteins or whole-cell lysates (WCLs) were separated by SDS-PAGE, transferred to 0.2-μm-pore-size polyvinylidene difluoride (PVDF) membrane (Bio-Rad), blocked for 1 h in 10% nonfat milk at room temperature, probed for the protein of interest overnight at 4°C, and visualized using HRP-conjugated secondary antibodies (1:10,000) with an Immun-Star WesternC chemiluminescence kit (Bio-Rad). To determine which of the three Shc and Ras genes are expressed in Daoy-TrkA cells, 25 or 50 μg of whole-cell lysates from Daoy-TrkA, HeLa cells, E18 (brain), P3 (brain), or P20 mouse cortex was separated by either 10 or 12% SDS-PAGE and analyzed as described above.

Confocal microscopy. Daoy-TrkA cells were seeded (50,000 cells) and cultured on 35-mm glass-bottomed dishes (MatTek Corporation) or poly-D-lysine-coated coverslips. The next day, cells were transfected with the appropriate expression plasmid (1 to 2 μg) mixed with Lipofectamine 2000 (Life Technologies) in 100 μl of serum-free Opti-MEM (Life Technologies) overnight or with a 1.5 ratio of Dreamfect Gold in 100 μl of serum-free Opti-MEM for 4 h. Fresh medium was provided, and cells were either left untreated or treated with NGF as indicated. To monitor latex bead uptake, cells were plated on 35-mm glass-bottom dishes and cotreated with 2 μl per ml of medium with an aqueous suspension of fluorescent red (excitation, 575 nm; emission 610 nm)-labeled latex beads (0.5 μm in diameter) (Sigma-Aldrich) and Alexa Fluor 488-dextran (5 μg/ml; Life Technologies) or Alexa Fluor 546-transferrin (10 μg/ml; Life Technologies) and Alexa Fluor 488-dextran (5 μg/ml; Life Technologies) prior to stimulation with 100 ng/ml NGF. Cells were visualized and captured with a Zeiss 510 Meta laser scanning confocal microscope using a 63× oil objective (optical section width of 0.7 μm).

Trypan blue exclusion assay. NGF-dependent cell death in Daoy-TrkA cells was quantified by trypan blue exclusion at 24 h following NGF stimulation. Cells were trypsinized and diluted 1:4 with 0.4% trypan blue solution, and the numbers of total cells and blue cells were counted by phase-contrast microscopy on a hemacytometer. All experiments were performed in triplicate.

Statistical analysis. All of the experiments were conducted at least three times. One-way analysis of variance (ANOVA) with Tukey multiple comparison tests was used to analyze the difference of means among each group. A P value of <0.05 is considered statistically significant.

RESULTS

TrkA generates large macropinosomes. To determine whether TrkA-induced macropinocytosis is distinct from receptor-mediated endocytosis, we employed two reporters, namely, Alexa Fluor 546-transferrin as a probe for receptor-mediated endocytosis and Alexa Fluor 488-dextran as a general tracer of fluid uptake via any mechanism. In the absence of NGF, we find significant colocalization of Alexa Fluor 488-dextran and Alexa Fluor 546-transferrin consistent with dextran being cointernalized with transferrin via endocytosis; however, in the presence of NGF, the bulk of Alexa Fluor 488-dextran (green) internalizes independent of Alexa Fluor 546-transferrin (red) into large (0.5-μm) macropinosomes (Fig. 1A). We then investigated the initial size of the vacuoles formed using Alexa Fluor 546-labeled latex beads and monitored their colocalization with Alexa Fluor 488-dextran. We found that cells could readily internalize 0.5-μm Alexa Fluor 546-labeled latex beads in response to NGF and that this showed significant colocalization with the Alexa Fluor 488-labeled dextran (Fig. 1B). By comparison, cells were not able to internalize 1.0-μm Alexa Fluor 488-labeled latex beads (data not shown).

Phosphatidylinositol 4-phosphate 5-kinase (PIP_5K) and phosphatidylinositol 3-kinase (PI3 kinase) participate in TrkA-induced macropinosome formation. We then initiated a series of experiments to characterize both the composition of the TrkA-induced macropinosome membranes as well as the signaling mechanism(s) that regulates their growth. We first determined whether TrkA-induced macropinosome membranes contain components identified in either constitutive or stimulated macropinosomes described in the literature, specifically, phosphatidylinositol 4,5-bisphosphate (PIP_2) and phosphatidylinositol 3,4,5-triphosphate (PIP_3) (15). We used EGFP-tagged constructs encoding the PH domain of AKT, which preferentially binds PIP_3 and to a lesser extent PIP_2, as well as the PH domain of phospholipase D which binds only PIP_2 (31). Cells transfected with EGFP alone showed diffuse green staining throughout the cell, and the macropinosome ruffles were not clearly identified (Fig. 1C); however, we found that both EGFP-tagged PH domain constructs were present within the macropinosome ruffles, indicating that both PIP_2 and PIP_3 are components of the initial lamellipodia

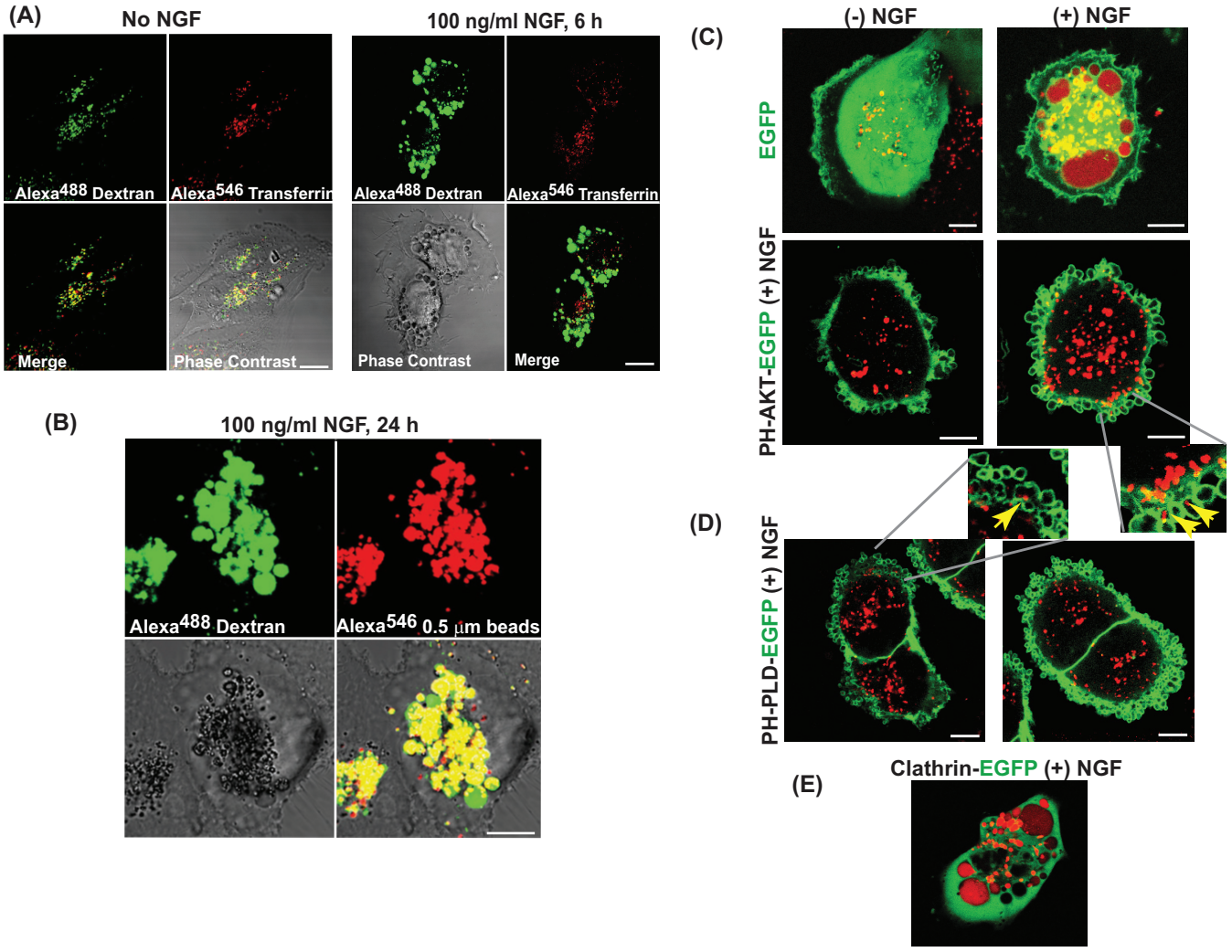

FIG 1 NGF-induced macropinosomes cointernalize dextran with 0.5-μm latex beads and contain both PIP_2 and PIP_3. Cells were cotreated with Alexa Fluor 546-transferrin and Alexa Fluor 488-dextran (A) or Alexa Fluor 488-dextran and 0.5-μm Alexa Fluor 546-latex beads (10 ng) (B) or transfected with EGFP alone or EGFP-tagged constructs encoding the PH domain of AKT (PIP_3 tracer) (C), the PH domain of PLD (PIP_2 tracer) (D), or EGFP-clathrin (E). Alexa Fluor 546-dextran was given as a fluid tracer, and cells were stimulated with 100 ng/ml NGF (24 h) and visualized by confocal microscopy. Scale bars, 10 μm.

(Fig. 1C and D). In fact, some of the initial macropinosomes contained Alexa Fluor 546-dextran (arrows) used as a fluid tracer. However, as the vacuoles internalized from the cell surface, both PH-AKT and PH-phospholipase D (PLD) were lost from the membrane, consistent with the fact that both PIP_2 and PIP_3 are lost during endocytosis (15). Consistent with our observation that NGF-dependent Alexa Fluor 488-dextran internalization was independent of receptor-mediated transferrin uptake (Fig. 1A), we found that EGFP-tagged clathrin did not label TrkA-induced macropinosomes (Fig. 1E).

TrkA stimulation causes activation of H-Ras and Rac. To define TrkA-dependent pathways that drive macropinocytosis, we focused on molecules that serve roles in clathrin-independent endocytosis and macropinocytosis-dependent actin remodeling. Collectively, these include PAK1, PI3 kinase, and Src (32), as well as several GTPases, including H-Ras, Cdc42, Rac1, Rab5, Arf1, Arf6, RhoA, and CtBP1/BARS (15, 16, 21, 33, 34, 35). With respect to Trk signaling, TrkA has been shown to activate H-Ras, Rap-1, Rac, and Cdc42 as well as to negatively regulate RhoA, depending on the cellular context (36–45). Thus, we first examined the NGF-induced activation kinetics of these GTPases using GST fusion proteins that contain binding domains of effector proteins that bind only the activated GTPases (PAK-1 for Rac and Cdc42, c-Raf-1 for H-Ras, Ral GDS for Rap1, and GGA3 for Arf6). Rac1 showed low basal activity in unstimulated cells and was weakly activated, as early as 10 min, in response to NGF (Fig. 2A). By comparison, there also were basal levels of H-Ras activation in unstimulated cells; however, in response to NGF, we observed a larger increase in H-Ras activation as early as 10 min, and this activation peaked at 6 h and remained elevated for up to about 12 h. Endogenous levels of H-Ras expression also remained constant during the 24-h period (Fig. 2B). When we directly compared activation levels of H-Ras relative to those of Rac, we found that Ras activation ranges from 3- to 7-fold while activation of Rac was less than 1-fold (Fig. 2C). By comparison, we found basal levels of Rap1, Cdc42, and Arf6 activation in unstimulated cells, and while Arf6 has never been shown to be activated by TrkA, it is activated downstream of some RTKs such as the Met (46) and

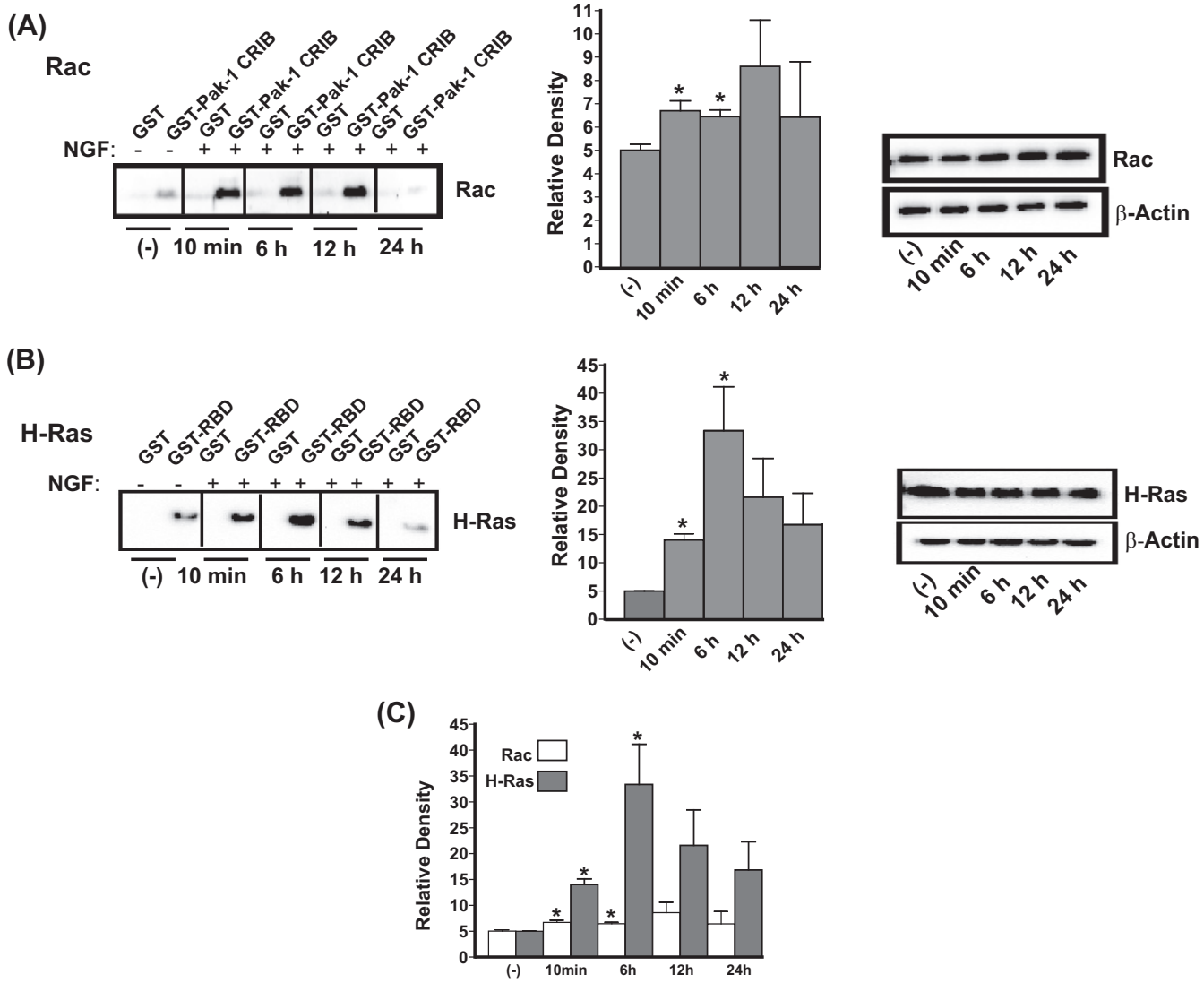

FIG 2 NGF-stimulated Daoy-TrkA cells activate both Rac and H-Ras. Daoy-TrkA cells were stimulated with 100 ng/ml NGF, and lysates were harvested at 10 min, 6 h, 12 h, and 24 h. (A and B) Lysates were assayed for activation of H-Ras and Rac using GST fusion proteins that bind only active Rac1 (Pak-1-CRIB) (A) and Ras (RBD) (B). Pulldown products (500 μg) and whole-cell lysates (WCLs) (25 μg) were analyzed on 12% SDS gels and Western blots probed with the indicated antibodies. WCLs were assayed for changes in the expression of each GTPase, relative to β-actin, at each time point. Changes in the activation of each GTPase were determined relative to levels of expression normalized to β-actin. (C) Direct comparison between the activation of Rac (less than 1-fold) relative to H-Ras (3- to 7-fold) during the same time period. Asterisks indicate a statistically significant ($P < 0.05$) increase relative to the level in unstimulated cells as performed using one-way ANOVA and a Tukey posttest.

muscle-specific kinase (MuSK) receptors (47), and it is involved in some forms of clathrin-independent endocytosis (15, 48). However, NGF did not stimulate any obvious change in the activation of Rap1, Cdc42, or Arf6 in Daoy-TrkA cells during the 24-h period of stimulation (see Fig. S1 in the supplemental material).

To complement the GTPase activation assays, we next determined whether dominant negative (DN) GTPase expression affected NGF-dependent macropinocytosis and found that DN-H-Ras and DN-Rab5 blocked NGF-induced macropinosomes, DN-Arf6 reduced the macropinosome size, while DN-Rap1b, -Rab7, -Rac1, -Arf1, -Rab34, -Dyn-2, -Cdc42, and -CtBP1/BARS had no effect (Fig. 3A). While NGF did not affect basal levels of Arf6 activation in Daoy-TrkA cells, the observation that DN-Arf6 reduced macropinosome size is consistent with the literature in that it traps activated H-Ras in recycling endosomes (49) and with our observation that DN-Arf6 generated small macropinosomes containing Alexa Fluor 546-dextran (Fig. 3A). The ability of DN-Rab5 to block NGF-induced macropinosomes is consistent with its known roles in mediating the early fusion of endosomes (15) and H-Ras-induced macropinosomes (49). With respect to DN-Rac1, as stated earlier, CA-Ras-dependent activation of macropinocytosis in U251 cells increased the pool of active Rac1 (21, 23), which is known to serve a role in membrane ruffling and the formation of lamellipodia (50, 51, 52). In contrast, we found that the levels of NGF-activated Rac1 in Daoy-TrkA cells were relatively low by 12 to 24 h (Fig. 2C), consistent with the fact that DN-Rac could not prevent TrkA-dependent macropinocytosis and that pretreatment of cells with the Rac-specific inhibitor

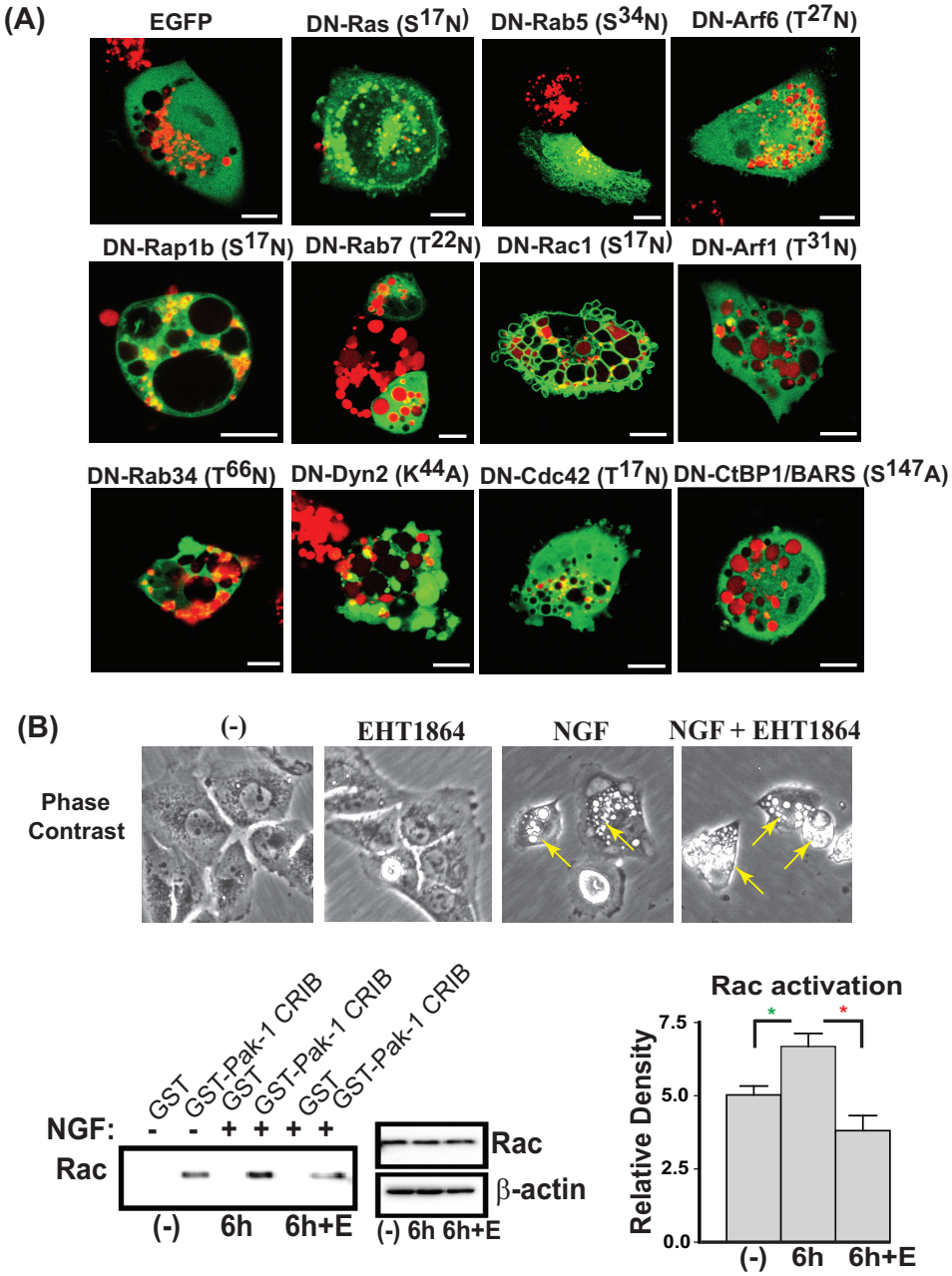

FIG 3 Expression of DN-H-Ras and Rab5 blocks and Arf6 reduces the size of NGF-induced macropinosomes. (A) EGFP-tagged DN GTPases (H-Ras, Arf6, Rab5, Rap1b, Rab7, Rac1, Arf1, Rab34, Dyn2, Cdc42, and CtBP1/BARS) were transfected into Daoy-TrkA cells and assayed for changes in both NGF-induced macropinosomes and the uptake of Alexa Fluor 546-dextran relative to cells transfected with EGFP at 24 h. Scale bars, 10 μm. (B) The Rac-specific inhibitor EHT1864 (10 μM) was assayed for changes in both NGF-induced vacuole formation at 24 h (phase-contrast microscopy) and changes in the activation of Rac at 6 h in a pulldown assay. Asterisks indicate a statistically significant ($P < 0.05$) increase in Rac activation at 6 h, relative to the level in unstimulated cells, as well as a significant decrease in activity in the presence of EHT1864, as determined using one-way ANOVA and a Tukey posttest.

EHT1864 (5 μM) did not block NGF-induced macropinosome formation despite its ability to block Rac1 activation at 6 h (Fig. 3B).

In a complementary approach, we then evaluated whether overexpression of constitutively active (CA) GTPases could drive NGF-independent macropinocytosis in Daoy cells (Fig. 4A). We found that overexpression of both CA-Ras and CA-Arf6 caused the generation of large vacuoles, consistent with macropinocytosis, and that CA-Rac1 generates small vacuoles while CA-Cdc42, CA-Rab34, and CA-Rap1b did not generate any. Since NGF did not stimulate any change in Arf6 activation, the CA-Arf6 vacuoles likely represent trapped vacuoles that cannot recycle back up to the membrane and subsequently fuse (15). Collectively, these observations suggest that H-Ras is the primary GTPase driving TrkA-dependent macropinosome formation. To test this hypothesis further, we addressed whether CA-Ras-induced macropinosomes could be blocked by the CK1-specific inhibitor D4476 (53), which we previously found to block TrkA-induced macropi-

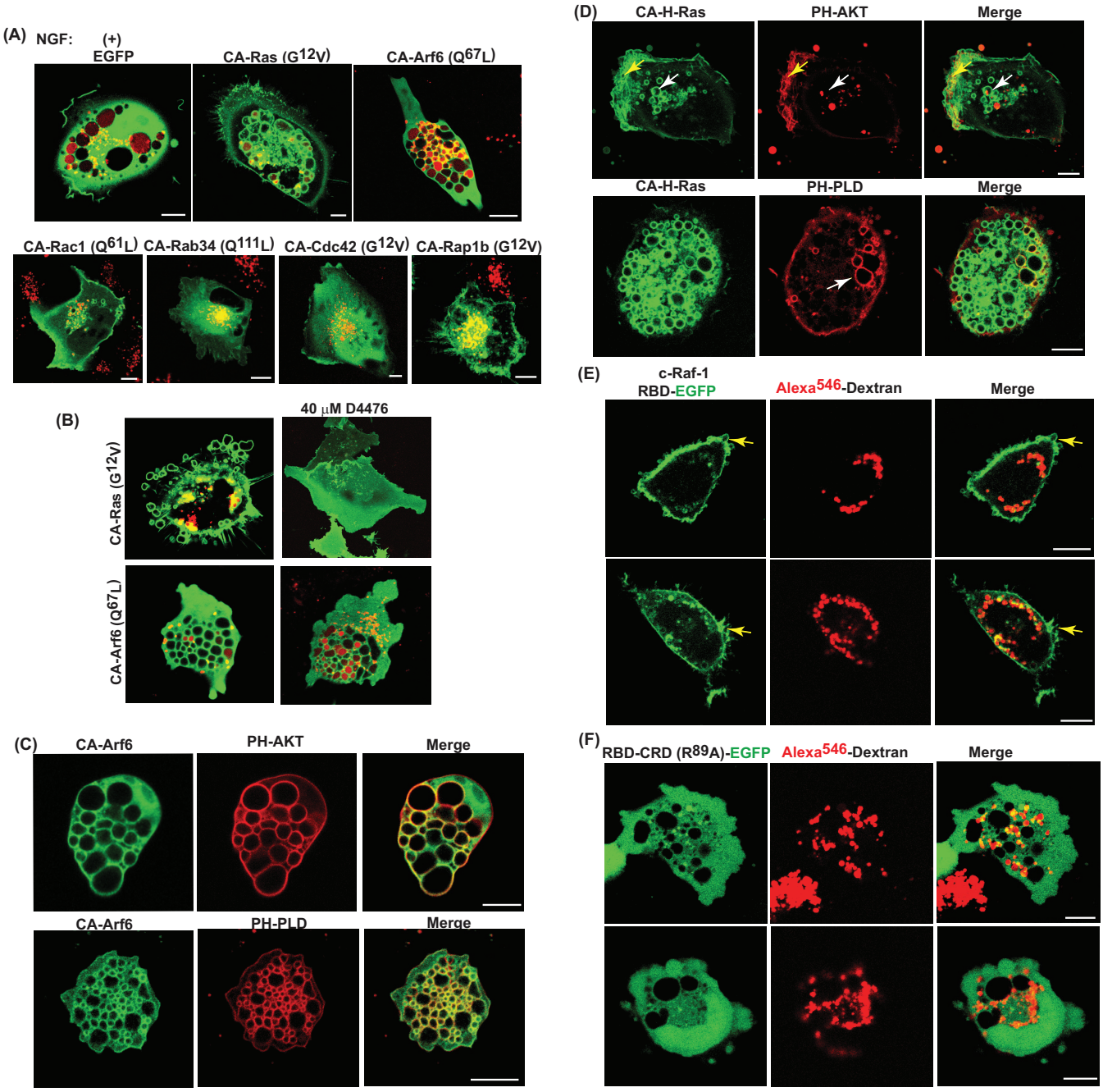

FIG 4 CA-Ras mimics NGF-induced macropinocytosis in Daoy-TrkA cells. (A) EGFP-tagged CA-Ras and CA-Arf6, but not CA-Rac1, Rab34, Cdc42, or Rap1b, induce NGF-independent macropinocytosis and Alexa Fluor 546-dextran uptake comparable to levels in cells transfected with EGFP and NGF stimulated (24 h). (B) Macropinosomes induced by CA-Ras-EGFP but not by CA-Arf6-EGFP are blocked by the CK1 inhibitor D4476. (C) CA-Arf6-EGFP-induced macropinosomes contain both PIP_3 (PH-AKT-mCherry) and PIP_2 (PH-PLD-mCherry). (D) The majority of CA-Ras-EGFP-induced macropinosomes do not contain PIP_3 (PH-AKT-mCherry) and/or PIP_2 (PH-PLD-mCherry) (white arrows). (E) EGFP-tagged RBD of c-Raf-1 localizes active Ras in the initial lamellipodia and the macropinosomes as well as in large, fused vacuoles in the presence of NGF. (F) The EGFP-tagged cRaf-1 CRD ($R^{89}A$) mutant, which cannot bind active Ras, is diffusely found throughout the cytosol in the presence of NGF. Scale bars, 10 μm.

nocytosis (13). As expected, we found that CA-Ras-induced but not CA-Arf6-induced macropinosomes could be completely blocked by D4476 (Fig. 4B). We further examined the phospholipid composition (PIP_2 and PIP_3) of CA-Arf6- and CA-Ras-induced macropinosomes compared to that of macropinosomes induced by TrkA by coexpressing EGFP-CA-Arf6 and CA-Ras with red fluorescent protein (RFP)-fused PH domains of AKT and PLD. We found that CA-Arf6 vacuoles contain both PIP_2/PIP_3 (Fig. 4C), consistent with previous reports showing that unless Arf6 is inactivated shortly after the initial stage of membrane internalization and PIP_2 is lost, the vacuoles are trapped and become progressively larger as they fuse (54). In contrast, we found that

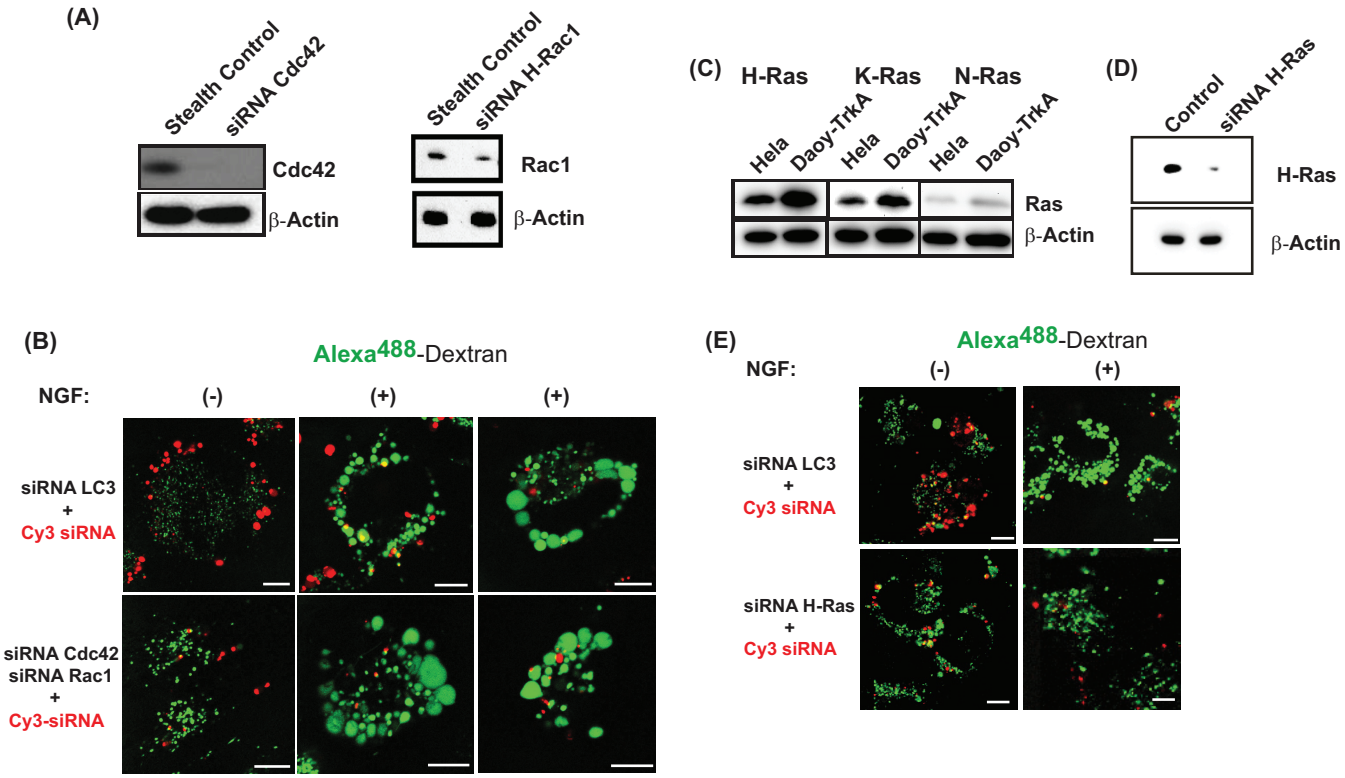

FIG 5 siRNA-mediated knockdown of H-Ras but neither Cdc42 nor Rac1 blocks NGF-induced macropinosomes. (A) Daoy-TrkA cells were transfected with siRNAs against Cdc42, Rac1, and a stealth control, and changes in protein expression were assayed by Western blotting at 48 h. (B) Daoy-TrkA cells were cotransfected with a Cy3 (red) control siRNA and either a nonspecific siRNA (LC3) or siRNAs against both Cdc42 and Rac1. Cells were either left unstimulated or treated with NGF, and changes in Alexa Fluor 488-dextran uptake were examined in Cy3-positive cells at 24 h. (C) Lysates from Daoy-TrkA cells were examined to determine if they express one or all three Ras isoforms relative to expression in HeLa cell lysates as a control. (D) siRNA to H-Ras effectively reduce H-Ras expression. (E) Daoy-TrkA cells were cotransfected with a Cy3 (red) control siRNA and either a nonspecific siRNA (LC3) or the H-Ras siRNA. Cells were either left unstimulated or treated with NGF, and changes in Alexa Fluor 488-dextran uptake were examined in Cy3-positive cells at 24 h. Scale bars, 10 μm.

while the initial CA-Ras-induced ruffles contained PIP_3, based on the costaining with EGFP-PH-AKT (Fig. 4D, yellow arrows), the internalized macropinosomes did not (Fig. 4D, white arrows). By comparison, while all of the CA-Arf6-induced macropinosomes still contained PIP_2, only a few of the CA-Ras-induced macropinosomes contained PIP_2 (Fig. 4D, white arrows). These observations are consistent with the lack of both AKT and PLD being localized to the large internal TrkA-induced macropinosomes (Fig. 1C and D) and further support the model that H-Ras is the primary GTPase driving this process. Consistent with this logic, the EGFP-tagged Ras binding domain (RBD) and cysteine-rich domain (CRD) of the effector protein c-Raf-1 labeled both the initial membrane ruffles as well as the enlarged vacuolar membranes (Fig. 4E, arrows). By comparison, an EGFP-tagged c-Raf-1 RBD-CRD mutant ($R^{89}A$), which can no longer bind activated H-Ras, was diffusely distributed in the cell (Fig. 4F) (55).

Knockdown of H-Ras prevents TrkA-induced macropinocytosis. To control against potential off-target effects generated by overexpressing DN constructs, we utilized siRNAs to deplete specific GTPases and assayed changes in NGF-induced macropinocytosis. Transfection of siRNAs for both Cdc42 and Rac1 effectively decreased their expression by 24 h relative to control siRNAs (Fig. 5A). However, when Daoy-TrkA cells were cotransfected with both siRNAs, along with a Cy3-labeled control siRNA to identify transfected cells, there was no apparent decrease in the size of the NGF-induced Alexa Fluor 488-dextran-containing vacuoles relative to sizes in cells transfected with a control siRNA (Fig. 5B). For Ras, we first determined which of the three Ras genes (Harvey [H], Kirsten [K], and/or neuroblastoma [N]) are expressed in Daoy-TrkA cells and found high levels of H-Ras and K-Ras and low levels of N-Ras (Fig. 5C). Given our overexpression studies with CA and DN-H-Ras, we first determined how changes in H-Ras expression alone would affect NGF-induced macropinosomes. Using an siRNA specific to H-Ras, we found that it effectively reduced endogenous expression of H-Ras (Fig. 5D) as well as the size of NGF-induced vacuoles in Cy3 (red)-positive cotransfected cells (Fig. 5E) relative to expression in cells transfected with siRNA controls.

The FRS2 adapter, not ShcA, is essential to TrkA-induced macropinosome formation. NGF activation of TrkA results in receptor dimerization, phosphorylation of the activation loop tyrosines, Tyr^{683}/Tyr^{684}, and subsequent phosphorylation of $Tyr^{490/499}$ in the juxtamembrane region. This enables competitive binding between the Shc and FRS2 adapters to $pTyr^{490}$ (27), and since both Shc and FRS2 are able to activate H-Ras (Fig. 6A), we determined which adapter is essential to this process. The Shc family of adapters includes four members (ShcA, -B, -C, and -D) (56). ShcA is highly expressed during embryogenesis and is expressed only in progenitor cells in the mature brain while ShcB/ShcC are primarily expressed after birth, and ShcD is primarily

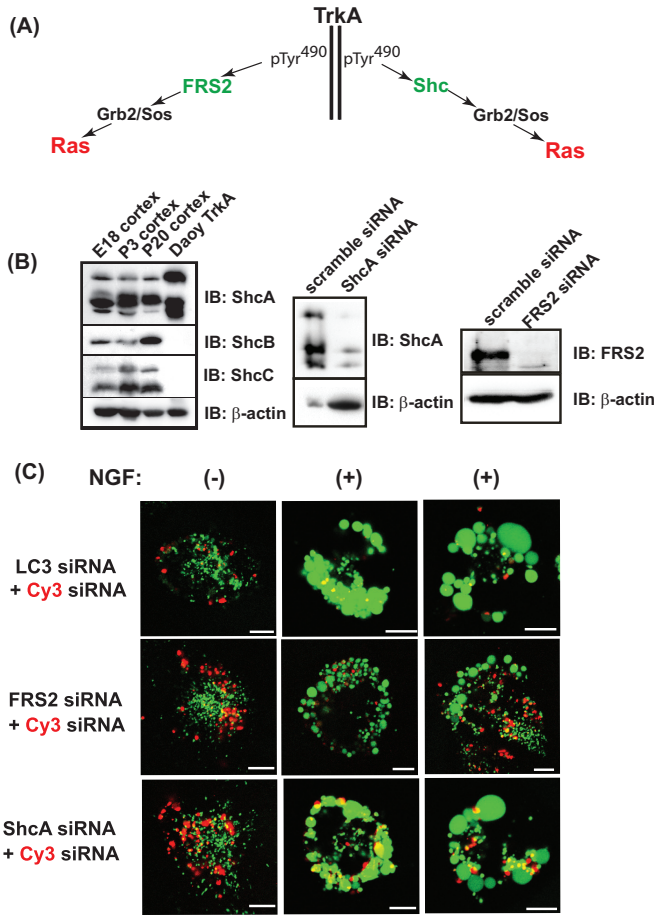

FIG 6 Binding of FRS2 but not ShcA to the phosphorylated juxtamembrane tyrosine residue Tyr^{490} is essential to H-Ras activation by TrkA. (A) Schematic showing that FRS2 and Shc bind competitively to $pTyr^{490}$ following TrkA activation. (B) Daoy-TrkA cells express ShcA but not ShcB or ShcC. siRNAs for both human ShcA and FRS2 effectively reduce expression of their respective targets in transfected Daoy-TrkA cells relative to the siRNA control. (C) Daoy-TrkA cells were cotransfected with a Cy3 control siRNA and either a nonspecific siRNA (LC3) or the siRNA against ShcA or FRS2. Cells were either left unstimulated or treated with NGF, and changes in Alexa Fluor 488-dextran uptake were examined in Cy3-positive cells at 24 h. Scale bars, 10 μm.

expressed outside the nervous system. We first determined which Shc adapters were expressed in Daoy-TrkA cells compared to expression in lysates prepared from E18, P3, and P20 mouse cortices. We found that Daoy-TrkA cells express only ShcA (Fig. 6B). Then we assayed FRS2/ShcA siRNAs for loss of expression in transfected Daoy-TrkA cells and found that both siRNAs effectively reduced expression of their target proteins relative to a scrambled siRNA control (Fig. 6B). Daoy-TrkA cells were then cotransfected with ShcA/FRS2 siRNAs, along with a Cy3-labeled siRNA control, and Cy3-positive cells were examined for changes in Alexa Fluor 488-dextran uptake relative to that in cells transfected with a control siRNA (LC3). Accordingly, we found that loss of FRS2 but not ShcA effectively reduced the size of NGF-induced macropinosomes, resulting in macropinosomes comparable to those observed in unstimulated cells (Fig. 6C).

Src kinase is essential to NGF-induced macropinosome formation. The soluble tyrosine kinase, Src, is another candidate signaling molecule that has been shown to be involved in membrane ruffling and macropinocytosis in different cellular contexts (32, 57, 58). Although the molecular mechanisms involved in Src-mediated macropinocytosis have not been fully elaborated, many of the pathways involve several downstream effectors such as PI3 kinase and phospholipase C as well as phospholipase D (15). Importantly, Src is known to be involved in TrkA-dependent signaling. Specifically, Src activation precedes the activation of H-Ras, and it is recruited into TrkA signaling via FRS2 (Fig. 7A) (26, 27, 59). In our initial studies to investigate whether Src was involved in NGF-induced macropinocytosis, we determined whether the Src inhibitor, PP2, affected the process. Interestingly, we found that 7.5 μM PP2 effectively reduced macropinocytosis to levels observed with vehicle alone (Fig. 7B) and that this concentration did not affect TrkA kinase activity (Fig. 7C). While higher concentrations of PP2 also blocked cell death, they impeded NGF-induced phosphorylation of the juxtamembrane $pTyr^{490}$ residue (Fig. 7C). Activation of Src involves the dephosphorylation of the self-inhibitory carboxyl-terminal tyrosine residue, Y^{527}, and phosphorylation of Y^{416} which resides in the activation loop (60, 61, 62). When we examined the kinetics of Src phosphorylation in response to NGF in Daoy-TrkA cells, we observed a significant increase in the amount of phosphorylation at Y^{416} by 6 h, which subsequently decayed over time (Fig. 7D), with little change in the phosphorylation state of Y^{527} (data not shown). Cotreatment with the CK1 inhibitor, D4476, did not affect the kinetics of Src activation (Fig. 7D, right panel), indicating that CK1 activation is either independent or downstream of Src. We then used siRNAs to address the role of Src expression/activation on NGF-induced macropinocytosis. An Src siRNA effectively reduced Src expression by 24 h, and this remained reduced up to 72 h posttransfection (Fig. 7E). Moreover, we found that cells cotransfected with Src siRNA plus a Cy3-labeled control siRNA showed a large reduction in the internalization of Alexa Fluor 488-dextran compared to that in cells transfected with control siRNAs and, in fact, internalized Alexa Fluor 488-dextran to levels similar to those in unstimulated cells (Fig. 7F). Finally, we expressed EGFP-tagged wild-type (WT) Src, as well as a DN-Src mutant (residues 1 to 516) (32), in Daoy-TrkA cells and determined how their expression affected NGF-induced macropinocytosis. The results demonstrate that overexpression of WT Src does localize to large macropinosomes in NGF-stimulated cells (Fig. 7G). In contrast, overexpression of DN-Src-GFP effectively blocks NGF-induced macropinosome formation (Fig. 7G).

Casein kinase 1 phosphorylation and inactivation of RhoB facilitate macropinocytosis. We next addressed the role of RhoB, another member of the Rho family of small GTPases which also includes RhoA and RhoC in macropinocytosis (63). RhoB is involved in a variety of cellular functions, including the organization and maintenance of actin stress fibers (64). Thus, we first analyzed cells for NGF-dependent changes in the activation of RhoB using a GST fusion construct encoding the Rho binding domain of the effector protein rhotekin. In contrast to all the other GTPases tested (Fig. 2; see also Fig. S1 in the supplemental material), we found a steady decrease in both the activation and expression levels of RhoB in response to NGF such that by 12 h, the amount of active RhoB was approximately half that observed at 6 h (Fig. 8A). In fact, no active RhoB was observed by 24 h though its levels of expression remained constant between 12 and 24 h (Fig. 8A). We then addressed whether inactivation of RhoB was essential to macropinosome formation and found that expression of CA-

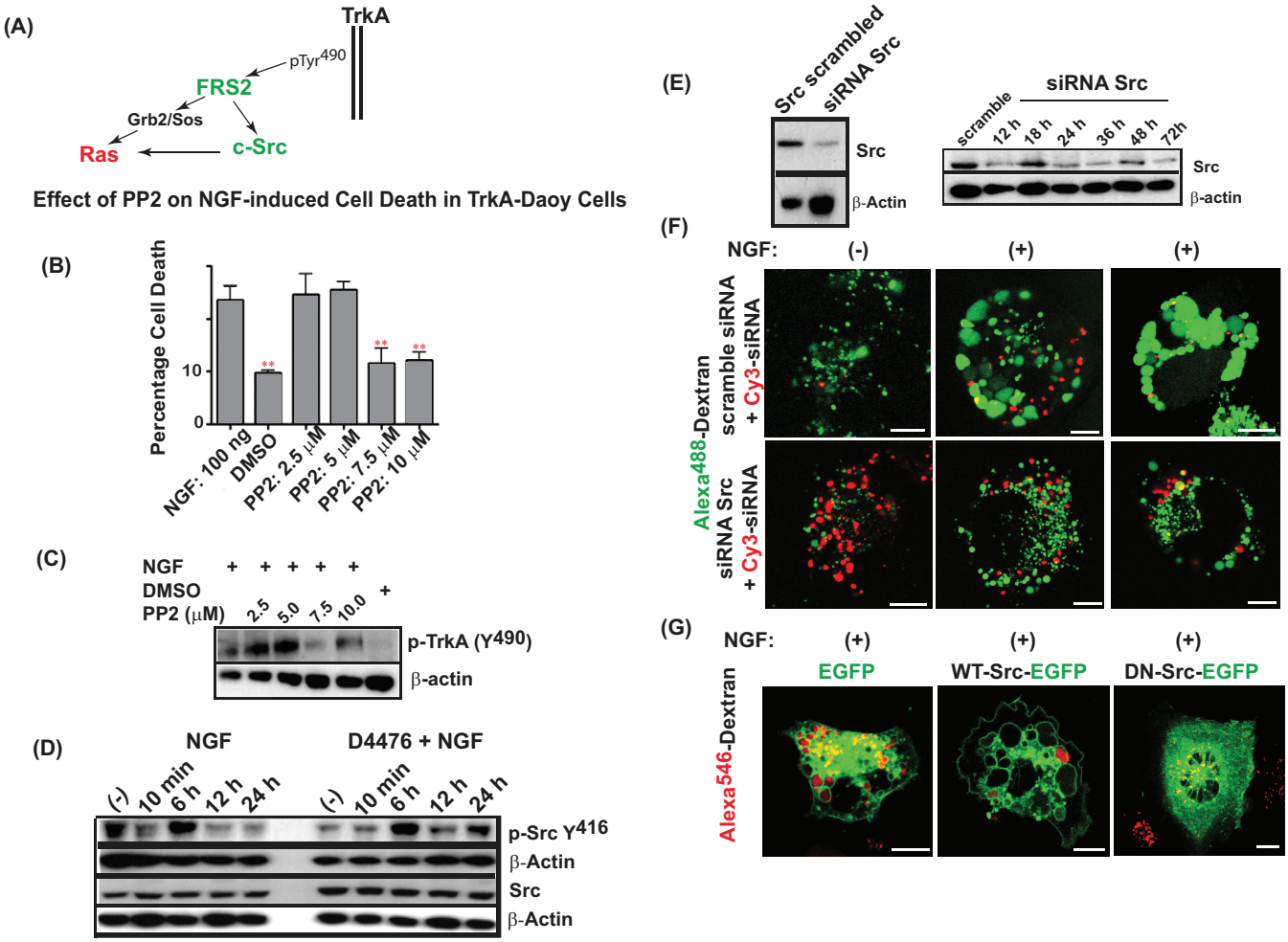

FIG 7 Src activation, via FRS2, is essential to NGF-dependent macropinocytosis and cell death. (A) Schematic showing that Src is recruited into TrkA signaling via FRS2, and this facilitates activation of H-Ras. (B) Daoy-TrkA cells were treated with PP2 or DMSO (1 h) prior to addition of NGF and incubated for an additional 12 h. Cells were scored for cell death using a trypan blue exclusion assay ($n = 3$). The asterisks represent a statistically significant decrease ($P < 0.05$) relative to the value for NGF-stimulated cells in the absence of inhibitor; values are comparable to that for control cells stimulated with DMSO alone. (C) Daoy-TrkA cells were treated as described in panel B, lysed, and analyzed by Western blotting for TrkA phosphorylation at pY^{490} relative to the β-actin level. (D) Daoy-TrkA cells were either left untreated or pretreated with D4476 (1 h) prior to NGF stimulation. Lysates were analyzed for changes in the phosphorylation status of Src (Y^{416}) relative to total levels of Src and β-actin. (E) Daoy-TrkA cells were transfected with an Src siRNA or an Src scramble control for 24 h (left panel) or up to 72 h (right panel), and changes in Src expression were determined by Western blotting relative to the level of β-actin. (F) Daoy-TrkA cells were cotransfected with a Cy3 control siRNA and either a scramble siRNA or the Src siRNA. Cells were either left unstimulated or treated with NGF, and changes in Alexa Fluor 488-dextran uptake were examined in Cy3-positive cells at 24 h. (G) Daoy-TrkA cells were transfected with EGFP-tagged WT or DN-Src and left untreated or stimulated with NGF and Alexa Fluor 546-dextran for 24 h prior to examining changes in macropinocytosis. Scale bars, 10 μm.

RhoB ($Q^{63}L$) and the maintenance of actin stress fibers effectively blocked NGF-induced macropinocytosis (Fig. 8B).

Previously, we showed that the CK1 inhibitor D4476 completely blocked NGF-induced macropinocytosis in Daoy-TrkA cells although the mechanism was not initially clear (13). However, Tillement et al. demonstrated that RhoB, but neither RhoA nor RhoC, is a direct target of CK1δ kinase activity *in vitro* (28). Specifically, they demonstrated that RhoB is phosphorylated at Ser^{185}, and this results in the inactivation of RhoB (28). Thus, we considered the possibility that the failure to inactivate RhoB and the maintenance of actin stress fibers underscore the inhibitory action of D4476. To address this, we examined how expression of an RhoB $S^{185}A$ mutant affects NGF-induced macropinocytosis. As this mutant is incapable of being phosphorylated at Ser^{185}, it should exert a similar effect as CA-RhoB ($Q^{63}L$) and block NGF-induced macropinosome formation. Consistent with this logic, we found that expression of the RhoB ($S^{185}A$) mutant did, in fact, completely block NGF-induced macropinocytosis (Fig. 8B). To complement these studies, we reduced RhoB expression by RNA siRNA transfection and observed enhanced macropinocytosis in response to NGF, indicating that loss of RhoB-dependent stress fibers are essential (Fig. 8C).

RhoA activation is essential to NGF-induced macropinosome formation. We have demonstrated that the primary GTPase driving NGF-induced macropinocytosis in Daoy-TrkA cells is H-Ras (Fig. 2 to 5). However, activation of H-Ras itself does not directly affect F-actin reorganization. Thus, we considered whether activation of RhoA, which is known to directly affect F-actin reorganization, was activated by NGF in Daoy-TrkA cells, whether it was localized to the macropinosome membranes, and

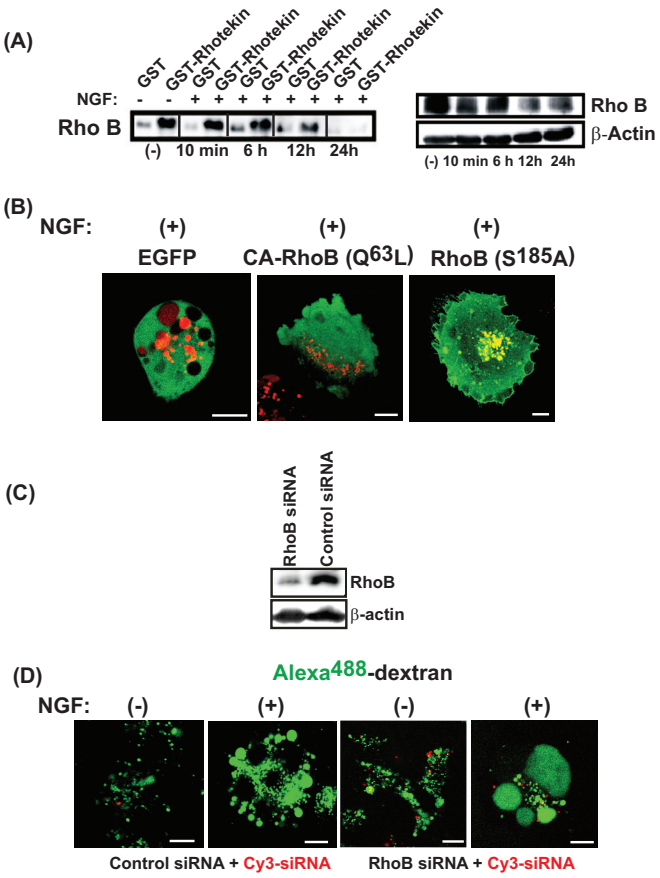

FIG 8 RhoB maintains actin stress fibers and must be inactivated via CK1-dependent phosphorylation at Ser^{185} to enable NGF-induced macropinocytosis. (A) Daoy-TrkA cells were stimulated with NGF, and lysates were harvested at 10 min, 6 h, 12 h, and 24 h and assayed for activation of RhoB using GST-rhotekin versus GST alone. Pulldown products and WCLs were analyzed on 12% SDS gels, and blots were probed with the indicated antibodies. WCLs were also assayed for changes in expression of RhoB, relative to the β-actin level, at each time point. (B) Daoy-TrkA cells were transfected with EGFP, EGFP-tagged CA-RhoB ($Q^{63}L$), and the EGFP-tagged site-directed RhoB mutant ($S^{185}A$). Cells were stimulated with NGF, and Alexa Fluor 546-dextran was added for 24 h before changes in macropinocytosis were examined. (C) Daoy-TrkA cells were transfected with control or RhoB siRNA, and changes in RhoB expression were examined by Western blotting at 24 h. (D) Cells were cotransfected with a Cy3 control siRNA and either a control siRNA or the RhoB siRNA. Cells were treated with NGF, and Alexa Fluor 488-dextran uptake was examined in Cy3-positive cells at 24 h. Scale bars, 10 μm.

whether it was essential to drive macropinocytosis. In this respect, RhoA activation has been shown to be associated with both neurite/dendritic extension and retraction in the nervous system (40, 65–69). We examined the kinetics of NGF-induced activation of RhoA in Daoy-TrkA cells using a GST fusion protein containing the Rho binding domain of rhotekin and observed RhoA activation as early as 10 min in response to NGF and peak activation at 6 h, and while the abundance of RhoA decreased by 12 to 24 h, the remaining molecules were still active (Fig. 9A). Next, we used a GFP-tagged reporter construct to visualize active RhoA (GFP-rGBD) and found that RhoA is diffusely distributed within the cytoplasm of unstimulated cells; however, following NGF stimulation, RhoA localized to the lamellipodia that initiate macropinocytosis, suggesting that it is the final GTPase stimulating F-actin reorganization (Fig. 9B). To confirm that RhoA activation is essential to NGF-induced macropinocytosis, we transfected Daoy-TrkA cells with YFP-tagged DN-RhoA ($T^{19}N$) and observed that it effectively blocked NGF-induced uptake of Alexa Fluor 546-dextran (Fig. 9C). Moreover, NGF-induced macropinosomes were effectively blocked by the Rho inhibitor CT04 (Fig. 9D). Collectively, these data confirmed that RhoA is the final GTPase regulating actin reorganization and macropinosome formation in response to NGF stimulation of Daoy-TrkA cells.

DISCUSSION

We previously demonstrated that TrkA-expressing Daoy cells undergo NGF-dependent macropinocytosis, resulting in cell death (13). Here, we have characterized the essential signaling cascade that drives this process. Specifically, it involves the recruitment of the FRS2 adaptor to activated TrkA and the subsequent activation of Src, H-Ras, and RhoA and the CK1-dependent inactivation of RhoB (Fig. 10). We found that macropinosomes are generated independently of receptor-mediated internalization, do not contain clathrin, and can be as large as 0.5 μm in size (Fig. 1). NGF-dependent cell death in Daoy-TrkA cells was strikingly similar to that observed in the GB cell line U251 following expression of activated H-Ras (20, 21, 23). Similar to findings in U251 cells, macropinocytosis in Daoy-TrkA cells is also dependent on the activation of H-Ras. Specifically, expression of DN-H-Ras (Fig. 3) and/or H-Ras siRNAs (Fig. 5D and E) completely blocked NGF-induced macropinocytosis. Conversely, macropinocytosis was induced in the absence of NGF by expression of CA-H-Ras (Fig. 4A), and CA-H-Ras-induced macropinosomes could be blocked with the CK1 inhibitor D4476 (Fig. 4B) that blocks NGF-induced macropinosomes (13). Finally, a construct encoding the Ras binding domain of c-Raf-1 (RBD-CRD) clearly demonstrated that active H-Ras was localized to the macropinosome membranes (Fig. 4E) in contrast to the diffuse staining throughout the cytosol observed with the EGFP-tagged c-Raf-1 RBD-CRD mutant ($R^{89}A$) that cannot bind activated H-Ras (Fig. 4F) (55). Collectively, these data all support the conclusion that H-Ras is the primary TrkA-coupled GTPase driving macropinocytosis. While H-Ras could be activated, via either Shc or FRS2, which competes for receptor binding following phosphorylation of the juxtamembrane tyrosine residue Y^{490} on TrkA (27) (Fig. 10), our studies demonstrate that FRS2 is the TrkA-dependent adapter essential to the process. Specifically, loss of FRS2 but not ShcA expression prevents NGF-induced macropinocytosis (Fig. 6). While activation of H-Ras is commonly associated with tumor cell growth and while many carcinomas arise as a result of mutations in H-Ras, it is important to note that activated H-Ras has never been reported as a cancer-causing oncogene in human brain tumors (24, 25). H-Ras has been shown to have a diversity of roles in different cell types, including inducing macropinocytosis to facilitate nutrient uptake in pancreatic tumors (14), in addition to its well-known roles in regulating cell survival (70), senescence (71), and cell death (72). As described earlier, H-Ras has been shown to stimulate macropinocytosis in U251 cells via activation of Rac1 (23), and expression of CA-Rac1 can itself stimulate macropinocytosis and cell death (21). This is in contrast to our observations that expression of CA-Rac1 had no effect on macropinosome formation and that the expression of DN-Rac1 and/or depletion of endogenous Rac1 by siRNA did not affect NGF-induced macropinocytosis. Moreover, while NGF induced a rapid increase in activated Rac1 that was sustained up to

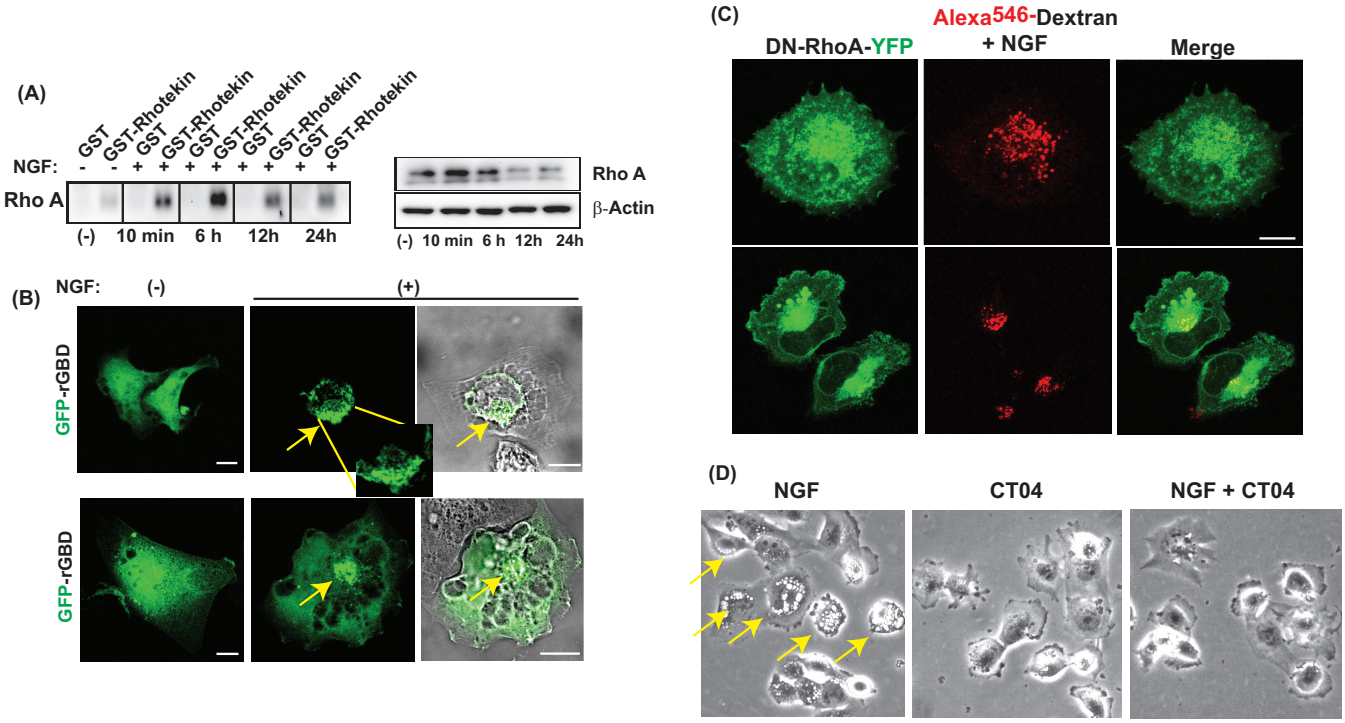

FIG 9 RhoA activation drives lamellipodium formation and is essential to NGF-induced macropinocytosis in Daoy-TrkA cells. (A) Daoy-TrkA cells were stimulated with NGF, and lysates were harvested at 10 min, 6 h, 12 h, and 24 h and assayed for activation of RhoA using GST-rhotekin versus GST alone. Pulldown products and WCLs were analyzed on 12% SDS gels, and blots were probed with the indicated antibodies. WCLs were also assayed for changes in expression of RhoA, relative to β-actin levels, at each time point. (B) Daoy-TrkA cells were transfected with an EGFP-tagged reporter construct encoding the RhoA binding domain of rhotekin to visualize active RhoA (GFP-rGBD). Cells were examined by confocal microscopy in the absence or presence of NGF stimulation at 24 h. (C) Daoy-TrkA cells were transfected with YFP-tagged DN RhoA ($T^{19}N$), treated with Alexa Fluor 546-dextran, stimulated with NGF, and visualized by confocal microscopy at 24 h. (D) Daoy-TrkA cells were treated with the Rho inhibitor CT04 (2 μg/ml) for 1 h prior to stimulation of cells with NGF for 4 h. Cells were visualized for macropinosomes by phase-contrast microscopy. Scale bars, 10 μm.

approximately 12 h, the increase in activation was less than 1-fold compared to the 3- to 7-fold increase in H-Ras activation during the same time period (Fig. 2C). While Rac1 is rapidly activated in response to NGF in PC12 cells and while it is necessary for Rho inactivation and the release of stress fibers to facilitate neurite outgrowth (44), we found that Rac1 activation was not essential for NGF-dependent macropinocytosis in Daoy-TrkA cells. In fact, the Rac-specific inhibitor EHT1864 had no effect on NGF-induced macropinocytosis, despite effectively blocking Rac activity (Fig. 3B).

Another small GTPase implicated in macropinocytosis and modulating actin dynamics and the endosomal recycling required for some types of clathrin-dependent and clathrin-independent endocytosis is Arf6 (15, 48, 73). Arf6 resides at the plasma membrane and when activated stimulates the accumulation of PIP_2 at the membrane through activation of phosphatidylinositol 4-phosphate 5 kinase (PIP_5K) and phospholipase D (PLD) (54, 74, 75), resulting in changes in the actin cytoskeleton (76). Following internalization of the endosome or macropinosome, Arf6 is inactivated, and PIP_2 is lost from the endosomal membrane (54) to be replaced by PIP_3 (49) generated by PI3 kinase (77). Under normal conditions where the macropinosome matures and is then recycled back up to the cell membrane, activation of Arf6 is again required for this final step and membrane fusion (54, 78). In U251 cells, the resting activity of Arf6 is high but drops significantly upon stimulation of macropinocytosis (23). In contrast to these results, we observed no change in the activation levels of Arf6 in NGF-stimulated Daoy-TrkA cells.

As has been observed in other cells (49, 54), expression of CA-Arf6 induced massive vacuolization similar to that observed with CA-H-Ras in Daoy-TrkA cells. However, the phosphatidylinositide composition of the CA-Arf6-induced macropinosomes is different from that induced by both NGF (Fig. 1) and CA-H-Ras (Fig. 4) in that CA-Arf6-induced macropinosomes result from the continual fusion of primary vacuoles due to the continued activation of PIP_5K and PLD (15, 54) and, as such, they are enriched in PIP_2 and PIP_3 (15, 48, 54).

Many of the proteins involved in macropinocytosis are downstream effectors of the nonreceptor tyrosine kinase Src. In fact, expression of CA-Src can induce the formation of membrane ruffles and macropinosomes in various cell types, including COS-7, HeLa, MDCK, and mouse embryonic fibroblast (MEFs) cells (32, 58, 79), and also induces rapid loss of actin stress fibers in MEFs (80). In addition, active Src associates with macropinosomes and remains associated through maturation up to fusion with lysosomes (32). We found that inhibition of Src by PP2 (7.5 μm) resulted in a reduction of macropinocytotic cell death in NGF-treated Daoy-TrkA cells, comparable to control levels, without affecting TrkA phosphorylation (Fig. 7B and C). Similarly, siRNA-mediated knockdown of Src led to a reduction in vacuole formation in the presence of NGF, comparable to the level in controls (Fig. 7E and F). In fact, overexpressing WT Src led to

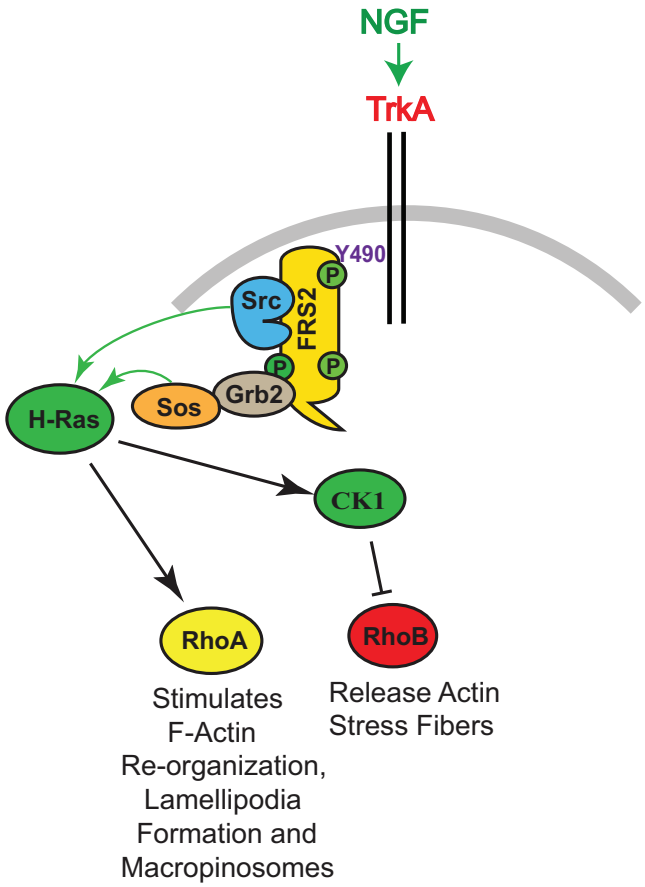

FIG 10 Schematic of TrkA-dependent signaling pathways that drive macropinocytosis.

larger NGF-induced macropinosomes in Daoy-TrkA cells, and Src was clearly localized on the internalized vacuoles, while expression of a DN mutant effectively blocked NGF-dependent macropinosomes (Fig. 7G). Src activation precedes the activation of H-Ras, is necessary for the sustained activation of extracellular signal-regulated kinase 1 and 2 (Erk1/2) essential to neurite outgrowth in PC12 cells (81, 82, 83), and is recruited into TrkA signaling via FRS2 (27) (Fig. 10).

The final steps in driving macropinocytosis requires membrane ruffling and lamellipodium formation that are dependent upon the relaxation of actin stress fibers, which enables actin to be remodeled (15, 16). Members of the Rho family of GTPases, in particular, RhoA, -B, and -C, have been shown to play important roles in the organization and maintenance of actin stress fibers (84). Our data indicate that relaxation of actin stress fibers, by CK1-dependent phosphorylation and inactivation of RhoB at residue Ser^{185}, is an essential initial requirement in the induction of macropinocytosis. How TrkA regulates the constitutive kinase activity of CK1 (85) and drives the phosphorylation of RhoB, downstream of H-Ras, remains to be clarified. In contrast, we found that activation of the related Rho family GTPase RhoA is essential to stimulate the actin reorganization and lamellipodial formation required to generate macropinosomes (Fig. 10). While RhoA has classically been thought to regulate only stress fiber formation, using fluorescent resonance energy transfer (FRET)-based reporters, Kurokawa and Matsuda demonstrated that RhoA is also highly activated in membrane ruffles and nascent lamellipodia in multiple cell lines in response to different stimuli (86). Using a GST fusion protein containing the Rho binding domain of rhotekin, we found RhoA highly activated in response to NGF, with peak activation at 6 h and lower levels of activation by 12 to 24 h (Fig. 9A). By using a reporter construct encoding the Rho binding domain of rhotekin to visualize active RhoA (GFP-rGBD), we found that active RhoA was diffusely distributed within the cytosol of unstimulated Daoy-TrkA cells, but in response to NGF, RhoA localized to the membrane ruffles and lamellipodia (Fig. 9B, arrows). Moreover, we found that expressing YFP-tagged DN-RhoA ($T^{19}N$) (Fig. 9C) as well treating Daoy-TrkA cells with the Rho inhibitor CT04 (Fig. 9D) effectively blocked NGF-induced macropinocytosis.

In summary, we have shown that macropinocytosis in Daoy-TrkA cells can be stimulated in the absence of NGF by expression of a CA mutant of H-Ras ($G^{12}V$). In addition, NGF-induced macropinocytosis is prevented in cells expressing a DN-H-Ras mutant ($T^{17}N$). In contrast to observations in glioblastoma U251 cells, we see no induction of macropinocytosis with a CA-Rac1 mutant ($Q^{61}L$) and conversely no protection against NGF-induced macropinocytosis in the presence of DN-Rac1 ($T^{17}N$). Other small GTPases such as Cdc42, while activated by the addition of NGF, do not appear to be essential in the initiation of macropinocytosis in Daoy-TrkA cells. Finally, inactivation of RhoB by phosphorylation at Ser^{185} by CK1 is fundamentally important in the induction of NGF-induced macropinocytosis. Inactivation of RhoB relaxes actin stress fibers and allows for actin remodeling and the formation of membrane ruffles and lamellipodia. Conversely, activated RhoA is the final and essential GTPase that reorganizes actin and generates the macropinosomes.

Considering the potential impact of these data, Vander Heiden et al. have reviewed the literature and discussed the fact that exploiting the Warburg effect, the reliance of most cancer cells on aerobic glycolysis and their need for large quantities of external nutrients to support biomass production, has been proposed as a general strategy to selectively kill cancer cells (87). Recently, for example, Yun et al. have demonstrated that colorectal cancer cells expressing K-RAS and B-RAF oncogenic mutants are selectively sensitive to high concentrations of vitamin C due to the overexpression of a glucose transporter GLUT1 in these cells, which takes up dehydroascorbic acid, ultimately causing accumulation of reactive oxygen species and cell death (88). Thus, the otherwise advantageous ability to take up more glucose actually makes these cells more susceptible to cell death. Macropinocytosis is a normal cellular process by which cells internalize extracellular fluids and nutrients from their environment and is one strategy that Ras-transformed cancer cells use to increase uptake of amino acids to meet the needs of rapid growth (14), but we have found that non-Ras-transformed medulloblastomas become susceptible to a TrkA-driven Ras-dependent uncontrolled macropinocytosis and tumor cell death (13). The links our studies provide here between TrkA and the regulation of GTPases and the resulting effects on actin cytoskeletal dynamics now provide the basis to test therapeutic strategies that target these pathways.

ACKNOWLEDGMENTS

We thank the many investigators who provided the following constructs for the experiments described here: M. Park (McGill University, Mon-

treal, Canada) for GST-GGA3; A. Richmond (Vanderbilt University, TN) for GST-RhoRBD and DN and CA RhoB; A. Hall (Sloane-Kettering, NY) for GST-PAK-CRIB; D. Shalloway (University of California, Berkeley, CA) for GST-Ras RBD; T. Balla (NIH, MD) for PH domains of AKT and PLCδ as well as the RBD-CRD domains of c-Raf-1 fused with EGFP; Y. Sako (RIKEN ASI, Japan) for the CRD c-Raf-1 $R^{89}A$ mutant; J. Donaldson (NIH, MD) for DN and CA-Arf6; P. Stork (Vollum Institute, OR) for DN and CA-Rap1b; N. Yamaguchi (Chiba University, Japan) for WT and DN Src; S. Ferguson (University of Ottawa, Ontario, Canada) for CA ($G^{12}V$) and DN ($T^{17}N$) Cdc42, DN ($S^{17}N$) Rac, DN ($K^{44}A$) dynamin 2, DN ($T^{31}N$) Arf1, DN ($N^{19}L$) RhoA, DN ($S^{34}N$) Rab5, DN ($T^{22}N$) Rab7, and EGFP-tagged clathrin; Alberto Luini (Institute of Protein Biochemistry, Naples, Italy) for DN ($S^{147}A$) CtBP1/BARS; T. Endo (Chiba University, Chiba, Japan) for DN ($T^{66}N$) and CA ($Q^{111}L$) Rab34; and A. Pradines (INSERM, France) for the RhoB ($S^{185}A$) mutant.

This research was supported with funds from an operating grant from the Cancer Research Society to S.O.M. and from the Canadian Institutes of Health Research to S.W.M. (MOP-GMX-93643) as well as from private donations.

S.O.M. conceived and supervised the project. C.L. performed confocal microscopy, cell culture, and biochemical experiments and data analyses. J.L., A.T., and J.I.S.M. performed cell culture and biochemical experiments and data analyses. C.S. performed confocal studies. S.H.P. and S.W.M. provided essential reagents and intellectual support.

We declare that we have no conflicts of interest.

FUNDING INFORMATION

This work, including the efforts of Stephen Michnick, was funded by Gouvernement du Canada | Canadian Institutes of Health Research (CIHR) (MOP-GMX-93643). This work, including the efforts of Susan O. Meakin, was funded by Cancer Research Society (CRS).

REFERENCES

1. **Kim JY, Sutton ME, Lu DJ, Cho TA, Goumnerova LC, Goritchenko L, Kaufman JR, Lam KK, Billet AL, Tarbell NJ, Wu J, Allen JC, Stiles CD, Segal RA, Pomeroy SL.** 1999. Activation of neurotrophin-3 receptor TrkC induces apoptosis in medulloblastomas. Cancer Res **59:**711–719.
2. **Brodeur GM.** 2003. Neuroblastoma: biological insights into a clinical enigma. Natue Rev Cancer **3:**203–216. http://dx.doi.org/10.1038/nrc1014.
3. **Marino S.** 2005. Medulloblastoma: developmental mechanisms out of control. Trends Mol Med **11:**17–22. http://dx.doi.org/10.1016/j.molmed.2004.11.008.
4. **Nakagawara A.** 2006. Neural crest development and neuroblastoma: the genetic and biological link. Prog Brain Res **146:**231–242.
5. **Brodeur GM, Minturn JE, Ho R, Simpson AM, Iyer R, Varela CR, Light JE, Kolla V, Evans AE.** 2009. Trk receptor expression and inhibition in neuroblastomas. Clin Cancer Res **15:**3244–3250. http://dx.doi.org/10.1158/1078-0432.CCR-08-1815.
6. **Gulino A, Arcella A, Giangaspero F.** 2008. Pathological and molecular heterogeneity of medulloblastoma. Curr Opin Oncol **20:**668–675. http://dx.doi.org/10.1097/CCO.0b013e32831369f4.
7. **Harel L, Costa B, Fainzilber M.** 2010. On the death Trk. Dev Neurobiol **70:**298–303. http://dx.doi.org/10.1002/dneu.20769.
8. **Thomaz A, Jaeger M, Buendia M, Bambini-Junior V, Gregianin LJ, Brunetto AL, Brunetto AT, de Farias CB, Roesler R.** 2016. BDNF/TrkB signaling as a potential novel target in pediatric brain tumors: anticancer activity of selective TrkB inhibition in medulloblastoma cells. J Mol Neurosci **59:**326–333. http://dx.doi.org/10.1007/s12031-015-0689-0.
9. **Chou TT, Trojanowski JQ, Lee VM.** 2000. A novel apoptotic pathway induced by nerve growth factor-mediated TrkA activation in medulloblastoma. J Biol Chem **275:**565–570. http://dx.doi.org/10.1074/jbc.275.1.565.
10. **Lavoie JF, LeSauteur L, Kohn J, Wong J, Furtoss O, Thiele CJ, Miller FD, Kaplan DR.** 2005. TrkA Induces apoptosis of neuroblastoma cells and does so via a p53-dependent mechanism. J Biol Chem **280:**29199–29207. http://dx.doi.org/10.1074/jbc.M502364200.
11. **Jung EJ, Kim DR.** 2008. Apoptotic cell death in TrkA-overexpressing cells: kinetic regulation of ERK phosphorylation and caspase-7 activation. Mol Cell **26:**12–17.
12. **Harel L, Costa B, Tcherpakov M, Zapatka M, Oberthuer A, Hansford LM, Vojvodic M, Levy Z, Chen Z-Y, Lee FS, Avigad S, Yaniv I, Shi L, Eils R, Fischer M, Brors B, Kaplan DR, Fainzilber M.** 2009. CCM2 mediates death signaling by the TrkA receptor tyrosine kinase. Neuron **63:**585–591. http://dx.doi.org/10.1016/j.neuron.2009.08.020.
13. **Li C, MacDonald JIS, Hryciw T, Meakin SO.** 2010. Nerve growth factor activation of the TrkA receptor induces cell death, by macropinocytosis, in medulloblastoma Daoy cells. J Neurochem **112:**882–889. http://dx.doi.org/10.1111/j.1471-4159.2009.06507.x.
14. **Commisso C, Davidson SM, Soydaner-Azeloglu RG, Parker SJ, Kamphorst JJ, Hackett S, Grabocka E, Nofal M, Drebin JA, Thompson CB, Rabinowitz JD, Metallo CM, Vander Heiden MG, Bar-Sagi D.** 2013. Macropinocytosis of protein is an amino acid supply route in Ras-transformed cells. Nature **497:**633–637. http://dx.doi.org/10.1038/nature12138.
15. **Donaldson JG, Porat-Shliom N, Cohen LA.** 2009. Clathrin-independent endocytosis: a unique platform for cell signaling and PM remodeling. Cell Signal **21:**1–6. http://dx.doi.org/10.1016/j.cellsig.2008.06.020.
16. **Lim JP, Gleeson PA.** 2011. Macropinocytosis: an endocytic pathway for internalising large gulps. Immunol Cell Biol **89:**836–843. http://dx.doi.org/10.1038/icb.2011.20.
17. **Lim J, Wang J, Kerr M, Teasdale R, Gleeson P.** 2008. A role for SNX5 in the regulation of macropinocytosis. BMC Cell Biol **9:**58. http://dx.doi.org/10.1186/1471-2121-9-58.
18. **Swanson JA, Watts C.** 1995. Macropinocytosis. Trends Cell Biol **5:**424–428. http://dx.doi.org/10.1016/S0962-8924(00)89101-1.
19. **Chi S, Kitanaka C, Noguchi K, Mochizuki T, Nagashima Y, Shirouzu M, Fujita H, Yoshida M, Chen W, Asai A, Himeno M, Yokoyama S, Kuchino Y.** 1999. Oncogenic Ras triggers cell suicide through the activation of a caspase-independent cell death program in human cancer cells. Oncogene **18:**2281–2290. http://dx.doi.org/10.1038/sj.onc.1202538.
20. **Kaul A, Overmeyer JH, Maltese WA.** 2007. Activated Ras induces cytoplasmic vacuolation and non-apoptotic death in glioblastoma cells via novel effector pathways. Cell Signal **19:**1034–1043. http://dx.doi.org/10.1016/j.cellsig.2006.11.010.
21. **Overmeyer JH, Kaul A, Johnson EE, Maltese WA.** 2008. Active Ras triggers death in glioblastoma cells through hyperstimulation of macropinocytosis. Mol Cancer Res **6:**965–977. http://dx.doi.org/10.1158/1541-7786.MCR-07-2036.
22. **Overmeyer J, Young A, Bhanot H, Maltese W.** 2011. A chalcone-related small molecule that induces methuosis, a novel form of non-apoptotic cell death, in glioblastoma cells. Mol Cancer **10:**69. http://dx.doi.org/10.1186/1476-4598-10-69.
23. **Bhanot H, Young AM, Overmeyer JH, Maltese WA.** 2010. Induction of nonapoptotic cell death by activated Ras requires inverse regulation of Rac1 and Arf6. Mol Cancer Res **8:**1358–1374. http://dx.doi.org/10.1158/1541-7786.MCR-10-0090.
24. **Fernandez-Medarde A, Santos E.** 2011. Ras in cancer and developmental diseases. Genes Cancer **2:**344–358. http://dx.doi.org/10.1177/1947601911411084.
25. **Parsons DW, Li M, Zhang X, Jones Sn Leary RJ, Lin JC-H, Boca SM, Carter H, Samayoa J, Bettegowda C, Gallia GL, Jallo GI, Binder ZA, Nikolsky Y, Hartigan J, Smith DR, Gerhard DS, Fults DW, VandenBerg S, Berger MS, Marie SKN, Shinjo SMO, Clara C, Phillips PC, Minturn JE, Biegel JA, Judkins AR, Resnick AC, Storm PB, Curran T, He Y, Rasheed BA, Friedman HS, Keir ST, McLendon R, Northcott PA, Taylor MD, Burger PC, Riggins GJ, Karchin R, Parmigiani G, Bigner DD, Yan H, Papadopoulos N, Vogelstein B, Kinzler KW, Velculescu VE.** 2011. The genetic landscape of the childhood cancer medulloblastoma. Science **331:**435–439. http://dx.doi.org/10.1126/science.1198056.
26. **Kremer NE, D'Arcangelo G, Thomas SM, DeMarco M, Brugge JS, Halegoua S.** 1991. Signal transduction by nerve growth factor and fibroblast growth factor in PC12 cells requires a sequence of src and ras. J Cell Biol **115:**809–819. http://dx.doi.org/10.1083/jcb.115.3.809.
27. **Meakin SO, MacDonald JIS, Gryz EA, Kubu CJ, Verdi JM.** 1999. The signaling adapter protein FRS-2 competes with Shc for binding to TrkA: a model for discriminating proliferation and differentiation. J Biol Chem **274:**9861–9870. http://dx.doi.org/10.1074/jbc.274.14.9861.
28. **Tillement V, Lajoie-Mazenc I, Casanova A, Froment C, Penary M, Tovar D, Marquez R, Monsarrat B, Favre G, Pradines A.** 2008. Phosphorylation of RhoB by CK1 impedes actin stress fiber organization and epidermal growth factor receptor stabilization. Exp Cell Res **314:**2811–2821. http://dx.doi.org/10.1016/j.yexcr.2008.06.011.
29. **Boukerche H, Su Z, Prévot C, Sarkar D, Fisher PB.** 2008. *mda-9/*

syntenin promotes metastasis in human melanoma cells by activating c-Src. Proc Natl Acad Sci U S A **105:**15914–15919. http://dx.doi.org/10.1073/pnas.0808171105.
30. **Deroanne CF, Hamelryckx D, Ho TTG, Lambert CA, Catroux P, Lapière CM, Nusgens BV.** 2005. Cdc42 downregulates MMP-1 expression by inhibiting the ERK1/2 pathway. J Cell Sci **118:**1173–1183. http://dx.doi.org/10.1242/jcs.01707.
31. **Kutateladze TG.** 2010. Translation of the phosphoinositide code by PI effectors. Nat Chem Biol **6:**507–513. http://dx.doi.org/10.1038/nchembio.390.
32. **Kasahara K, Nakayama Y, Sato I, Ikeda K, Hoshino M, Endo T, Yamaguchi N.** 2007. Role of Src-family kinases in formation and trafficking of macropinosomes. J Cell Physiol **211:**220–232. http://dx.doi.org/10.1002/jcp.20931.
33. **Liberali P, Kakkonen E, Turacchio G, Valente C, Spaar A, Perinetti G, Böckmann RA, Corda D, Colanzi A, Marjomaki V, Luini A.** 2008. The closure of PAK1-dependent macropinosomes requires the phosphorylation of CtBP1/BARS. EMBO J **27:**970–981. http://dx.doi.org/10.1038/emboj.2008.59.
34. **Swanson JA.** 2008. Shaping cups into phagosomes and macropinosomes. Nat Rev Mol Cell Biol **9:**639–649. http://dx.doi.org/10.1038/nrm2447.
35. **Doherty GJ, McMahon HT.** 2009. Mechanisms of endocytosis. Annu Rev Biochem **78:**857–902. http://dx.doi.org/10.1146/annurev.biochem.78.081307.110540.
36. **Talebian A, Robinson-Brookes K, MacDonald JIS, Meakin SO.** 2013. Ras guanine nucleotide releasing factor 1 (RasGrf1) enhancement of Trk receptor mediated neurite outgrowth requires activation of both H-Ras and Rac. J Mol Neurosci **49:**38–51. http://dx.doi.org/10.1007/s12031-012-9847-9.
37. **Valdez G, Akmentin W, Philippidou P, Kuruvilla R, Ginty DD, Halegoua S.** 2005. Pincher-mediated macroendocytosis underlies retrograde signaling by neurotrophin receptors. J Neurosci **25:**5236–5247. http://dx.doi.org/10.1523/JNEUROSCI.5104-04.2005.
38. **Chakrabarti K, Lin R, Schiller NI, Wang Y, Koubi D, Fan Y-X, Rudkin BB, Johnson GR, Schiller MR.** 2005. Critical role for kalirin in nerve growth factor signaling through TrkA. Mol Cell Biol **25:**5106–5118. http://dx.doi.org/10.1128/MCB.25.12.5106-5118.2005.
39. **York RD, Yao H, Dillon T, Ellig CL, Eckert SP, McClecksy EW, Stork PJ.** 1998. Rap1 mediates sustained MAP kinase activation induced by nerve growth factor. Nature **392:**622–626. http://dx.doi.org/10.1038/33451.
40. **Jeon C-Y, Moon M-Y, Kim J-H, Kim H-J, Kim J-G, Li Y, Jin J-K, Kim P-H, Kim H-C, Meier KE, Kim Y-S, Park J-B.** 2012. Control of neurite outgrowth by RhoA inactivation. J Neurochem **120:**684–698. http://dx.doi.org/10.1111/j.1471-4159.2011.07564.x.
41. **Aoki K, Nakamura T, Matsuda M.** 2004. Spatio-temporal regulation of Rac1 and Cdc42 activity during nerve growth factor-induced neurite outgrowth in PC12 Cells. J Biol Chem **279:**713–719. http://dx.doi.org/10.1074/jbc.M306382200.
42. **Ahmed I, Calle Y, Iwashita S, Nur-E-Kamal A.** 2006. Role of Cdc42 in neurite outgrowth of PC12 cells and cerebellar granule neurons. Mol Cell Biochem **281:**17–25. http://dx.doi.org/10.1007/s11010-006-0165-9.
43. **Kozma R, Sarner S, Ahmed S, Lim L.** 1997. Rho family GTPases and neuronal growth cone remodelling: relationship between increased complexity induced by Cdc42Hs, Rac1, and acetylcholine and collapse induced by RhoA and lysophosphatidic acid. Mol Cell Biol **17:**1201–1211. http://dx.doi.org/10.1128/MCB.17.3.1201.
44. **Nusser N, Gosmanova E, Zheng Y, Tigyi G.** 2002. Nerve growth factor signals through TrkA, phosphatidylinositol 3-kinase, and Rac1 to inactivate RhoA during the initiation of neuronal differentiation of PC12 Cells. J Biol Chem **277:**35840–35846. http://dx.doi.org/10.1074/jbc.M203617200.
45. **Nakamura T, Komiya M, Sone K, Hirose F, Gotoh N, Morii H, Ohta Y, Mori M.** 2002. Grit, a GTPase-activating protein for the Rho family, regulates neurite extension through association with the TrkA receptor and N-Shc and CrkL/Crk adapter molecules. Mol Cell Biol **22:**8721–8734. http://dx.doi.org/10.1128/MCB.22.24.8721-8734.2002.
46. **Parachoniak Christine A, Luo Y, Abella Jasmine V, Keen James H, Park M.** 2011. GGA3 functions as a switch to promote Met receptor recycling, essential for sustained ERK and cell migration. Dev Cell **20:**751–763. http://dx.doi.org/10.1016/j.devcel.2011.05.007.
47. **Luiskandl S, Woller B, Schlauf M, Schmid JA, Herbst R.** 2013. Endosomal trafficking of the receptor tyrosine kinase MuSK proceeds via clathrin-dependent pathways, Arf6 and actin. FEBS J **280:**3281–3297. http://dx.doi.org/10.1111/febs.12309.
48. **Donaldson JG, Jackson CL.** 2011. ARF family G proteins and their regulators: roles in membrane transport, development and disease. Nat Rev Mol Cell Biol **12:**362–375. http://dx.doi.org/10.1038/nrm3117.
49. **Porat-Shliom N, Kloog Y, Donaldson JG.** 2008. A Unique platform for H-Ras signaling involving clathrin-independent endocytosis. Mol Biol Cell **19:**765–775.
50. **Ridley AJ.** 2001. Rho family proteins: coordinating cell responses. Trends Cell Biol **11:**471–477. http://dx.doi.org/10.1016/S0962-8924(01)02153-5.
51. **Doughman RL, Firestone AJ, Wojtasiak ML, Bunce MW, Anderson RA.** 2003. Membrane ruffling requires coordination between type Iα phosphatidylinositol phosphate kinase and Rac signaling. J Biol Chem **278:**23036–23045. http://dx.doi.org/10.1074/jbc.M211397200.
52. **Wells CM, Walmsley M, Ooi S, Tybulewicz V, Ridley AJ.** 2004. Rac1-deficient macrophages exhibit defects in cell spreading and membrane ruffling but not migration. J Cell Sci **117:**1259–1268. http://dx.doi.org/10.1242/jcs.00997.
53. **Bain J, Plater L, Elliott M, Shpiro N, Hastie CJ, McLauchlan H, Klevernic I, Arthur JSC, Aless DR, Cohen P.** 2007. The selectivity of protein kinase inhibitors: a further uptake. Biochem J **408:**297–315. http://dx.doi.org/10.1042/BJ20070797.
54. **Brown FD, Rozelle AL, Yin HL, Balla T, Donaldson JG.** 2001. Phosphatidylinositol 4,5-bisphosphate and Arf6-regulated membrane traffic. J Cell Biol **154:**1007–1018. http://dx.doi.org/10.1083/jcb.200103107.
55. **Hibino K, Shibata T, Yanagida T, Sako Y.** 2011. Activation kinetics of RAF protein in the ternary complex of RAF, RAS-GTP, and kinase on the plasma membrane of living cells: single-molecule imaging analysis. J Biol Chem **286:**36460–36468. http://dx.doi.org/10.1074/jbc.M111.262675.
56. **Wills MKB, Jones N.** 2012. Teaching an old dogma new tricks: twenty years of Shc adaptor signalling. Biochem J **447:**1–16. http://dx.doi.org/10.1042/BJ20120769.
57. **Veithen A, Amyere M, Van Der Smissen P, Cupers P, Courtoy PJ.** 1998. Regulation of macropinocytosis in v-Src-transformed fibroblasts: cyclic AMP selectively promotes regurgitation of macropinosomes. J Cell Sci **111:**2329–2335.
58. **Mettlen M, Platek A, Van Der Smissen P, Carpentier S, Amyere M, Lanzetti L, De Diesbach P, Tyteca D, Courtoy PJ.** 2006. Src triggers circular ruffling and macropinocytosis at the apical surface of polarized MDCK cells. Traffic **7:**589–603. http://dx.doi.org/10.1111/j.1600-0854.2006.00412.x.
59. **Wooten MW, Seibenhener ML, Mamidipudi V, Diaz-Meco MT, Barker PA, Moscat J.** 2001. The atypical protein kinase C-interacting protein p62 is a scaffold for NF-κB activation by nerve growth factor. J Biol Chem **276:**7709–7712. http://dx.doi.org/10.1074/jbc.C000869200.
60. **Roskoski J, R.** 2005. Src kinase regulation by phosphorylation and dephosphorylation. Biochem Biophys Res Commun **331:**1–14. http://dx.doi.org/10.1016/j.bbrc.2005.03.012.
61. **Chellaiah MA, Schaller MD.** 2009. Activation of Src kinase by protein-tyrosine phosphatase-PEST in osteoclasts: comparative analysis of the effects of bisphosphonate and protein-tyrosine phosphatase inhibitor on Src activation in vitro. J Cell Physiol **220:**382–393. http://dx.doi.org/10.1002/jcp.21777.
62. **Mandal A, Shahidullah M, Beimgraben C, Delamere NA.** 2011. The effect of endothelin-1 on Src-family tyrosine kinases and Na, K-ATPase activity in porcine lens epithelium. J Cell Physiol **226:**2555–2561. http://dx.doi.org/10.1002/jcp.22602.
63. **Wennerberg K, Der CJ.** 2004. Rho-family GTPases: it's not only Rac and Rho (and I like it). J Cell Sci **117:**1301–1312. http://dx.doi.org/10.1242/jcs.01118.
64. **Raftopoulou M, Hall A.** 2004. Cell migration: Rho GTPases lead the way. Dev Biol **265:**23–32. http://dx.doi.org/10.1016/j.ydbio.2003.06.003.
65. **Maekawa M, Ishizaki T, Boku S, Watanabe N, Fujita A, Iwamatsu A, Obinata T, Ohashi K, Mizuno K, Narumiya S.** 1999. Signaling from Rho to the actin cytoskeleton through protein kinases ROCK and LIM-kinase. Science **285:**895–898. http://dx.doi.org/10.1126/science.285.5429.895.
66. **Feltrin D, Pertz O.** 2012. Assessment of Rho GTPase signaling during neurite outgrowth. Methods Mol Biol **827:**181–194. http://dx.doi.org/10.1007/978-1-61779-442-1_13.
67. **Sun Y, Lim Y, Li F, Liu S, Lu J-J, Haberberger R, Zhong J-H, Zhou X-F.** 2012. ProBDNF collapses neurite outgrowth of primary neurons by activating RhoA. PLoS One **7:**e35883. http://dx.doi.org/10.1371/journal.pone.0035883.

68. **Wills Zachary P, Mandel-Brehm C, Mardinly Alan R, McCord Alejandra E, Giger Roman J, Greenberg Michael E.** 2012. The Nogo receptor family restricts synapse number in the developing hippocampus. Neuron **73:**466–481. http://dx.doi.org/10.1016/j.neuron.2011.11.029.
69. **Zhao CF, Liu Y, Ni YL, Yang JW, Hui HD, Sun ZB, Liu SJ.** 2013. SCIRR39 promotes neurite extension via RhoA in NGF-induced PC12 cells. Dev Neurosci **35:**373–383. http://dx.doi.org/10.1159/000350715.
70. **Manning BD, Cantley LC.** 2007. AKT/PKB signaling: navigating downstream. Cell **129:**1261–1274. http://dx.doi.org/10.1016/j.cell.2007.06.009.
71. **Serrano M, Lin AW, McCurrach ME, Beach D, Lowe SW.** 1997. Oncogenic Ras provokes premature cell senescence associated with accumulation of p53 and p16INK4a. Cell **88:**593–602. http://dx.doi.org/10.1016/S0092-8674(00)81902-9.
72. **Overmeyer JH, Maltese WA.** 2011. Death pathways triggered by activated Ras in cancer cells. Front Biosci **16:**1693–1713. http://dx.doi.org/10.2741/3814.
73. **D'Souza-Schorey C, Chavrier P.** 2006. ARF proteins: roles in membrane traffic and beyond. Nat Rev Mol Cell Biol **7:**347–358. http://dx.doi.org/10.1038/nrm1910.
74. **Naslavsky N, Weigert R, Donaldson JG.** 2004. Characterization of a nonclathrin endocytic pathway: membrane cargo and lipid requirements. Mol Biol Cell **15:**3542–3552. http://dx.doi.org/10.1091/mbc.E04-02-0151.
75. **Funakoshi Y, Hasegawa H, Kanaho Y.** 2011. Regulation of PIP5K activity by Arf6 and its physiological significance. J Cell Physiol **226:**888–895. http://dx.doi.org/10.1002/jcp.22482.
76. **Ferrari C, Zippel R, Martegani E, Gnesutta N, Carrera V, Sturani E.** 1994. Expression of two different products of CDC25Mm, a mammalian Ras activator, during development of mouse brain. Exp Cell Res **210:**353–357. http://dx.doi.org/10.1006/excr.1994.1048.
77. **Engelman JA, Luo J, Cantley LC.** 2006. The evolution of phosphatidylinositol 3-kinases as regulators of growth and metabolism. Nat Rev Genet **7:**606–619. http://dx.doi.org/10.1038/nrg1879.
78. **Jovanovic OA, Brown FD, Donaldson JG.** 2006. An effector domain mutant of Arf6 implicates phospholipase D in endosomal membrane recycling. Mol Biol Cell **17:**327–335.
79. **Donepudi M, Resh MD.** 2008. c-Src trafficking and co-localization with the EGF receptor promotes EGF ligand-independent EGF receptor activation and signaling. Cell Signal **20:**1359–1367. http://dx.doi.org/10.1016/j.cellsig.2008.03.007.
80. **Saito Y, Tsuzuki K, Yamada N, Okado H, Miwa A, Goto F, Ozawa S.** 2003. Transfer of NMDAR2 cDNAs increases endogenous NMDAR1 protein and induces expression of functional NMDA receptors in PC12 cells. Mol Brain Res **110:**159–168. http://dx.doi.org/10.1016/S0169-328X(02)00548-X.
81. **Obara Y, Labudda K, Dillon TJ, Stork PJS.** 2004. PKA phosphorylation of Src mediates Rap1 activation in NGF and cAMP signaling in PC12 cells. J Cell Sci **117:**6085–6094. http://dx.doi.org/10.1242/jcs.01527.
82. **Arthur DB, Akassoglou K, Insel PA.** 2006. P2Y2 and TrkA receptors interact with Src family kinase for neuronal differentiation. Biochem Biophys Res Commun **347:**678–682. http://dx.doi.org/10.1016/j.bbrc.2006.06.141.
83. **Tsuruda A, Suzuki S, Maekawa T, Oka S.** 2004. Constitutively active Src facilitates NGF-induced phosphorylation of TrkA and causes enhancement of the MAPK signaling in SK-N-MC cells. FEBS Lett **560:**215–220. http://dx.doi.org/10.1016/S0014-5793(04)00115-2.
84. **Spiering D, Hodgson L.** 2011. Dynamics of the Rho-family small GTPases in actin regulation and motility. Cell Adhesion Migration **5:**170–180. http://dx.doi.org/10.4161/cam.5.2.14403.
85. **Knippschild U, Gocht A, Wolff S, Huber N, Löhler J, Stöter M.** 2005. The casein kinase 1 family: participation in multiple cellular processes in eukaryotes. Cell Signal **17:**675–689. http://dx.doi.org/10.1016/j.cellsig.2004.12.011.
86. **Kurokawa K, Matsuda M.** 2005. Localized RhoA activation as a requirement for the induction of membrane ruffling. Mol Biol Cell **16:**4294–4303. http://dx.doi.org/10.1091/mbc.E04-12-1076.
87. **Vander Heiden MG, Cantley LC, Thompson CB.** 2009. Understanding the Warburg effect: the metabolic requirements of cell proliferation. Science **324:**1029–1033. http://dx.doi.org/10.1126/science.1160809.
88. **Yung Yun C, Stoddard Nicole C, Mirendil H, Chun J.** 2015. Lysophosphatidic acid signaling in the nervous system. Neuron **85:**669–682. http://dx.doi.org/10.1016/j.neuron.2015.01.009.